Redox Biology 26 (2019) 101307

Contents lists available at ScienceDirect

Redox Biology

journal homepage: www.elsevier.com/locate/redox

Research Paper

Mitochondrial calcium uniporter regulates PGC-1α expression to mediate metabolic reprogramming in pulmonary fibrosis

Linlin Gu[a], Jennifer L. Larson Casey[a], Shaida A. Andrabi[b], Jun Hee Lee[b], Selene Meza-Perez[c], Troy D. Randall[c], A. Brent Carter[a,d,*]

[a] Department of Medicine, Division of Pulmonary, Allergy and Critical Care Medicine, University of Alabama at Birmingham, Birmingham, AL, 35294, USA
[b] Department of Pharmacology & Toxicology, University of Alabama at Birmingham, Birmingham, AL, 35294, USA
[c] Department of Medicine, Division of Clinical Immunology and Rheumatology, University of Alabama at Birmingham, Birmingham, AL, 35294, USA
[d] Birmingham VAMC, Birmingham, AL, 35294, USA

ARTICLE INFO

Keywords:
MCU
PGC-1α
Metabolic reprogramming
Fatty acid oxidation (FAO)
Mitochondrial ROS
Pulmonary fibrosis

ABSTRACT

Idiopathic pulmonary fibrosis (IPF) is a progressive disease with an increased mortality. Metabolic reprogramming has a critical role in multiple chronic diseases. Lung macrophages expressing the mitochondrial calcium uniporter (MCU) have a critical role in fibrotic repair, but the contribution of MCU in macrophage metabolism is not known. Here, we show that MCU regulates peroxisome proliferator-activated receptor gamma coactivator 1-alpha (PGC-1α) and metabolic reprogramming to fatty acid oxidation (FAO) in macrophages. MCU regulated PGC-1α expression by increasing the phosphorylation of ATF-2 by the p38 MAPK in a redox-dependent manner. The expression and activation of PGC-1α via the p38 MAPK was regulated by MCU-mediated mitochondrial calcium uptake, which is linked to increased mitochondrial ROS (mtROS) production. Mice harboring a conditional expression of dominant-negative MCU in macrophages had a marked reduction in mtROS and FAO and were protected from pulmonary fibrosis. Moreover, IPF lung macrophages had evidence of increased MCU and mitochondrial calcium, increased phosphorylation of ATF2 and p38, as well as increased expression of PGC-1α. These observations suggest that macrophage MCU-mediated metabolic reprogramming contributes to fibrotic repair after lung injury.

1. Introduction

The prevalence of pulmonary fibrosis is increasing to nearly 80 per 100,000 annually, and the cost of care has had a significant upward trend [1,2]. The disease is devastating with the average life expectancy of 3–5 years after diagnosis for certain forms of pulmonary fibrosis, such as idiopathic pulmonary fibrosis (IPF) [1,3]. IPF, a progressive interstitial pneumonia, is the most common form of pulmonary fibrosis and is most commonly associated with aging [4]. In contast, other types of pulmonary fibrosis, such as that associated with collagen vascular disease, can occur at an early age. Although other types of pulmonary fibrosis can occasionally have the histologic feature of usual interstitial pneumonia (UIP) at end-stage, the presence of UIP on histology is required for the diagnosis of IPF, which appears as a “honeycomb” on radiographic images. The presence of UIP is associated with the rapid progression of the dysregulated fibrotic repair. Unlike other forms of pulmonary fibrosis, the etiology of IPF is poorly understood. The incidence and mortality from IPF is increasing worldwide, with an estimated 40,000 lives lost in the U.S. each year [1,5]. The recently approved therapies for IPF reduce the rate of decline in lung function; however, neither drug is associated with improvements in quality of life or changes in survival [6,7].

The mitochondrial calcium uniporter (MCU) is a highly selective ion channel that transports calcium into the mitochondrial matrix to initiate multiple enzymatic processes. MCU is critical for cellular signaling, energy status, and survival. The physiological or pathological necessity of MCU in various organ functions or diseases is well-described. For example, MCU is necessary for heart rate acceleration, and inhibition of MCU reduced inappropriate heart rate increases without affecting resting heart rate [8]. MCU is also required in controlling mitochondrial calcium uptake in skeletal muscle to prevent muscle atrophy [9]. In early brain injury after subarachnoid hemorrhage, mitochondrial calcium concentration and oxidative stress was MCU-dependent, and inhibition of MCU abrogated oxidative stress and brain

* Corresponding author. Department of Medicine, Division of Pulmonary, Allergy and Critical Care Medicine, University of Alabama at Birmingham, Birmingham, AL, 35294, USA.
E-mail address: bcarter1@uab.edu (A.B. Carter).

https://doi.org/10.1016/j.redox.2019.101307
Received 24 June 2019; Received in revised form 19 August 2019; Accepted 20 August 2019
Available online 25 August 2019

injury after hemorrhage [10]. Moreover, MCU is required in the progression of triple-negative breast cancer by modulating mtROS production and HIF-1α expression, thereby enhancing glycolytic metabolism that is utilized by malignant cells [11]. These studies suggest that MCU and mitochondrial calcium uptake is a potential novel therapeutic target; however, the role of MCU and mitochondrial Ca^{2+} in fibrosis, especially pulmonary fibrosis, is not fully understood.

Metabolic reprogramming is a hallmark in multiple diseases. Studies examining the relationship of MCU to metabolic reprogramming are limited. MCU expression is increased in adipose tissue of obese subjects and in insulin-resistant adipocytes [12]. This increased expression affects mitochondrial metabolism that is linked to obesity development by inducing a pro-inflamatory and an oxidative state. In contrast, the level of MCU expression is decreased in cardiac myocytes in response to hyperglycemia. The reduced expression diminished glycolysis and increased fatty acid oxidation (FAO) [13]. The loss of MCU does not alter basal metabolism; however, it impairs the ability of cells to respond to stress [14], which typically occurs in disease states. For example, breast cancer cells do not rely on MCU for survival [15], but MCU contributes significantly to cell growth and metastasis by enhancing mitochondrial bioenergetics [11].

Here, we show that MCU-mediated metabolic reprogramming to FAO in lung macrophages was regulated by increasing mitochondrial ROS (mtROS) to induce transcriptional activation of PGC-1α by phosphorylation of ATF2 via the p38 MAPK. Moreover, expression of dominant-negative MCU in macrophages protected mice from fibrosis development via metabolic reversal to glycolysis.

2. Materials and methods

2.1. Human subjects

The Institutional Review Board of the University of Alabama at Birmingham approved the protocol of obtaining lung macrophages from normal and idiopathic pulmonary fibrosis (IPF) subjects. Normal participants had to meet the following criteria: 1) age between 30 and 75 years old; 2) no history of cardiopulmonarydisease or other chronic disease; 3) no prescription or non-prescription medication except oral contraceptives; 4) no recent or current evidence of infection; and 5) lifetime nonsmoker. The IPF subjects had to meet the following criteria: 1) forced vital capacity had to be at least 50% predicted; 2) current nonsmoker; 3) no recent or current evidence of infection; 4) evidence of restrictive physiology on pulmonary function tests; and 5) usual interstitial pneumonia on chest computed tomography scans. Fiberoptic bronchoscopy with bronchoalveolar lavage (BAL) was performed after subjects received local anesthesia. Three subsegments of the lung were lavaged with five 20-ml aliquots of normal saline, and the first aliquot in each was discarded. The percentage of lung macrophages was determined by Wright-Giemsa stain and varied from 90 to 98%.

2.2. Mice

Wild-type (WT) and *DN-MCU-Lyz2-cre* mice were littermates, and the genotype was confirmed using tail DNA. The *DN-MCU-Lyz2-cre* mice, which harbor overexpression of a dominant-negative form of MCU (*DN-MCU*) in lung macrophages, were generated by crossing *DN-MCU$^{fl/fl}$* mice (a generous gift from Dr. Mark E. Anderson, Johns Hopkins University, Baltimore, MD, USA) with *Lyz2-cre* mice. *Tgfb1$^{-/-}$Lyz2-cre* mice have been described previously [16]. Mice were 8-12-week-old, and an equal number of male and female mice were chosen for exposures.

Reciprocal bone marrow chimeric mice were generated by irradiating recipient mice twice (separated by 4 h) with 450 rads from an X-ray source. Immediately following the second dose of irradiation, the recipients were intravenously administered 1×10^7 total bone marrow cells from donor mice and allowed to reconstitute for at least 8 weeks prior to any experiment. Irradiated mice were maintained on medicated diet, Mod LabDiet® 5P00 with 0.025%Trimethoprim and 0.124% Sulfamethoxazol (TestDiet, St. Louis, MO), for 4 weeks after irradiation and returned to normal chow for the remaining time. Bleomycin was used to expose mice intratracheally (*i.t*) at a concentration of 1.75 U/kilogram. All protocols were approved by the University of Alabama at Birmingham Institutional Animal Care and Use Committee.

2.3. Plasmids, small interfering RNAs, and transfections

pFIV-CMV-MCU_{WT} and pFIV-CMV-MCU_{DN} were generous gifts from Dr. Mark E. Anderson. pCDNA3.1-MCU_{WT} was generated by ligating mouse MCU gene open reading frame (ORF) into pcDNA™3.1/V5-His TOPO vector (Invitrogen# K480001). The MCU ORF was amplified by PCR using cDNA template. pcDNA3.1-MCU_{DN} was derived from pCDNA3.1-MCU_{WT} by site-directed mutation of two sites (D260Q and E263Q) using Q5 Site-Directed Mutagenesis Kit (NEB# E0552S). pCDNA4-PGC-1α was purchased from Addgene (#10974). The pcDNA-MKK6(Glu) and pCMV-Flag-$p38_{DN}$ plasmids have been previously described (a generous gift from Dr. Roger Davis, University of Massachusetts, Worcester, MA) [17,18]. MCU shRNA plasmid was purchased from Sigma-Aldrich (SHCLNG-NM_001033259), and the corresponding empty vector pLKO.1 puro was attained from Addgene (8453). pcDNA3.1-catalase was generated by ligating human catalase gene ORF into pcDNA™3.1/V5-His TOPO vector (Invitrogen# K480001). Plasmids were transfected with X-treme Gene 9 Transfection Reagent (Roche# 06365809001), according to the manufacturer's manual. After 24 h, cells were subjected to either treatment of specific interest or collected for downstream purposes.

Mouse PGC-1α siRNA (CD.Ri.24068.13.9, Integrated DNA Technologies) and mouse Cpt1a siRNA (mm.Ri.Cpt1a.13.1, IDT) were transfected using DharmaFECT 4 (Dharmacon# T-2004), according to the manufacturer's protocol. Human Rieske siRNA [16] was transfected with DharmaFECT 2 (Dharmacon# T-2002). Co-transfections of siRNAs with a plasmid at the same time was performed using DharmaFECT Duo (Dharmacon# T-2010).

2.4. Mitochondrial membrane potential (ΔΨm) determination

Measurement of ΔΨm was performed with JC-1 (Invitrogen #T3168) staining according to the manufacturer's protocol. Cells were rinsed once in 1 × DPBS and labelled with JC-1 (10 μg/ml) for 20 min at 37 °C. Cells were then washed three times with warm HBSS with Ca^{2+}/Mg^{2+} and subjected to imaging. Both monomer (green) and aggregate (red) images were captured under confocal microscopy to reflect the changes in ΔΨm. To quantitate ΔΨm, equal amout of cells were labled with JC-1 probe as above indicated. Fluorescence was measured by using a SpectraMax M2 platereader (monomer: excitation at 514 nm and emission at 525 nm; aggregate: excitation at 585 nm and emission at 595 nm). Carbonyl cyanide m-chlorophenylhydrazone (CCCP, 3 μM) was used as a positive control.

2.5. Oxygen consumption rate (OCR) determination

OCR was determined by using a Seahorse XF96 bioanalyzer (Seahorse Bioscience). In brief, cells were placed in an XF96 cell culture microplate (Seahorse Bioscience) at 7×10^4 cells/well. The plate was subjected to OCR measurement in the bioanalyzer with sequential additions of oligomycin (final at 2 μM), carbonyl cyanide 3-chlorophenylhydrazone (CCCP, final at 1.5 μM) and rotenone (final at 1 μM). FAO was assayed in either MH-S cells or primary lung macrophages by measuring OCR in the Seahorse bioanalyzer with addition of the FAO substrate, palmitate-BSA (final of 167 μM palmitate in 28.3 μM BSA), or BSA control (final at 28.3 μM). MH-S cells were incubated overnight in substrate-limited medium before the OCR measurement the following day. Primary lung macrophages were incubated for at least 30 min in

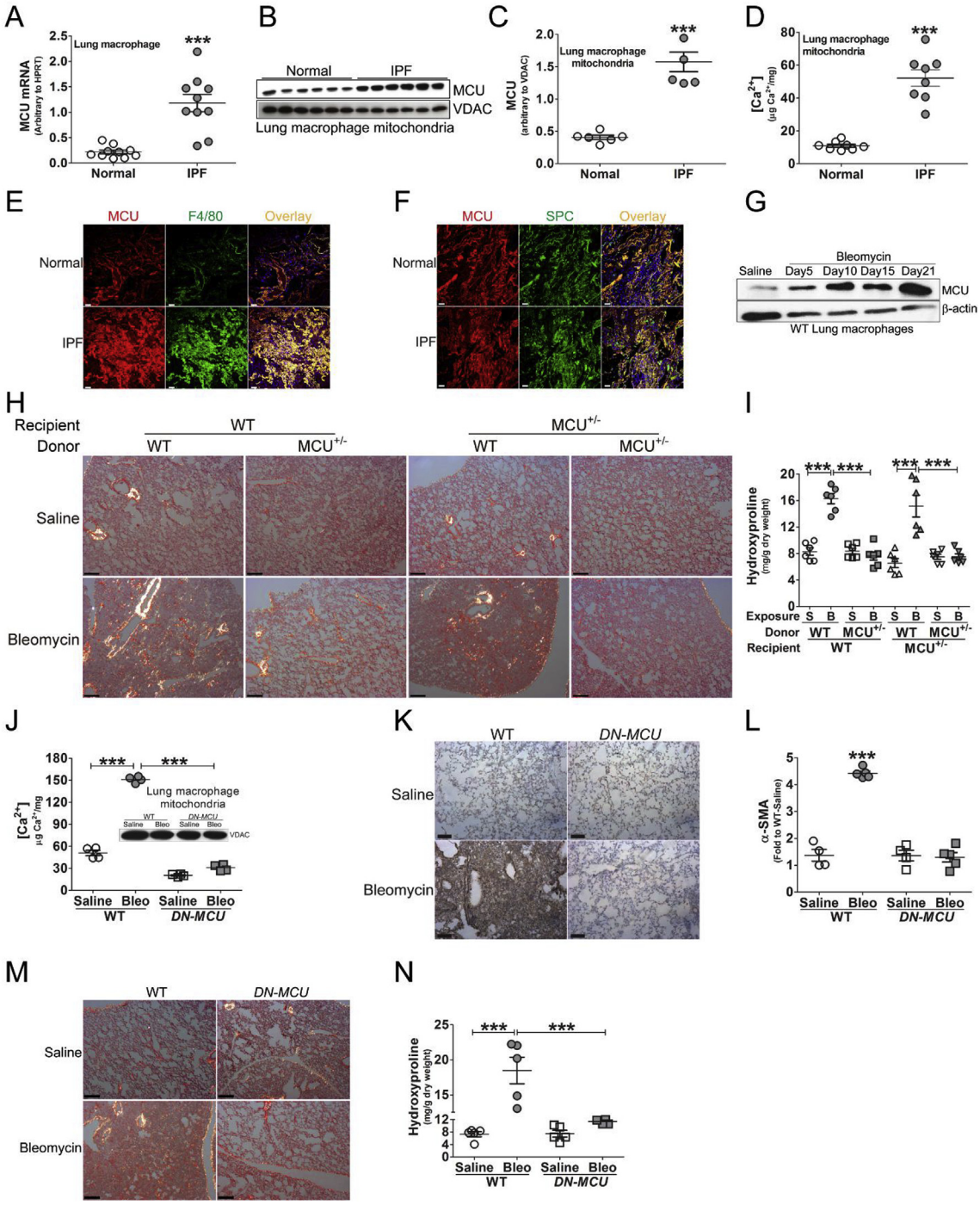

Fig. 1. MCU expression and mitochondrial Ca^{2+} are increased in IPF lung macrophages.

(A) Total RNA was isolated from lung macrophages of normal or IPF subjects. MCU mRNA was measured by real-time PCR, $n = 10$. (B) MCU was detected by immunoblot analysis in lung macrophage mitochondria from human subjects. (C) Statistical analysis, $n = 6$. (D) Ca^{2+} was measured in isolated mitochondria of lung macrophages from human subjects, $n = 8$. (E) The colocalization of MCU and F4/80 in lung tissue of normal and IPF subjects was detected by IHC-P. Representative micrograph of three individual subjects. Scale bars, 20 μm. (F) The colocalization of MCU and SPC in lung tissue from normal and IPF subjects was detected by IHC-P. Representative micrograph of three individual subjects. Scale bars, 20 μm. (G) WT mice were exposed to saline or bleomycin (1.75U/kg). Lung macrophages were harvested by BAL at indicated time points (day 5, 10, 15 and 21). Whole cell lysate was prepared for the detection of MCU by immuoblot analysis. (H) Reciprocal bone marrow (BM) chimera was performed with WT and MCU $^{\pm}$ mice. After 8 weeks mice were exposed to saline or bleomycin (1.75U/kg) for 21 days. Lungs were subjected to Sirius red staining. Represented micrographs from 6 mice per condition are shown. Scale bars, 200 μm at x5. (I) Lung collagen content was determined by hydroxyproline assay, $n = 6$. WT and *DN-MCU-Lyz2-cre* littermates were exposed to saline or bleomycin for 21 days. (J) Mitochondrial Ca^{2+} in lung macrophages from mice was measured in freshly isolated mitochondria, $n = 4$. (K) α-SMA expression was determined in lung tissue by IHC-P. Representative micrograph of four individual replicates. Scale bars, 200 μm at x5. (L) Quantification of α-SMA expression in mice lung tissue, $n = 4$ (saline) and $n = 5$ (bleomycin). (M) Representative ($n = 5$) microphaph of Sirius red staining of lung parenchyma, scale bars, 200 μm at x5 and (N) hydroxyproline assay, $n = 5$. All data are expressed as mean ± SEM. S, saline; B and Bleo, bleomycin; *DN-MCU*, *DN-MCU-Lyz2-cre*. One-way ANOVA with Tukey's post hoc comparison (I, J, L and N). Two-tailed student's *t*-test (A, C and D). ***$p \leq 0.001$. See also Fig. S1.

the substrate-limited medium to ensure sufficient adherence to the microplate. Cells were then placed in FAO assay medium, and palmitate:BSA or BSA control was added before measuring OCR.

2.6. IHC-P

Lung tissues of experimental mice or human subjects, fixed in 10% formalin and embeded in parrifin, were sectioned to 4 or 10 μm thickness. The tissue slides were deparaffinized by incubating at 60 °C for 30 min and 2× wash in xylene for 5 min each. The tissue slides were rehydrated with a graded series of ethanol incubation (absolute, 95%, 90%, 80% and 70% in ddw; 3 min each grade). The tissues were subjected to antigen unmasking with 1 mM EDTA in ddw, pH 8.0 (sub-boiling temperature, 40 min). To quench the endogeneous peroxidase activity, tissue slides were washed 3× in ddw (3 min each) and incubated in 3% H_2O_2 for 10 min, followed by 2× wash in ddw (5 min each) and 2× wash in TBST (5 min each). The slides were blocked at room temperature for 1 h with PBS containing 10% BSA and 10% normal goat serum.

To detect α-SMA by chromogenic staining, the slides were incubated with mouse anti-SMA (American Research products#03-61001) in the 5× diluted blocking solution (4 °C, overnight). The slides were then washed and incubated with SignalStain Boost Detection Reagent (CellSignaling#8125) at room temperature for 30 min, followed by staining with the Signal Stain DAB substrate kit (CellSignaling#8059). The slides were then immersed in ddw to stop reaction, and subjected to counterstain with hematoxylin (Vector Labs#H-3404).

To detect MCU, F4/80, and SPC by immunofluorescent staining, tissue slides were incubated with mastermix of mouse anti-MCU (Sigma#AMAB91189) and rabbit anti-F4/80 (Thermo Fisher#PA5-32399) or mastermix of mouse anti-MCU (Sigma#AMAB91189) and rabbit anti-SPC (Millipore#AB3786). Secondary antibodies were mastermix of goat anti-mouse IgG-TRITC and goat anti-rabbit IgG-FITC. Slides were then counterstained with DAPI.

2.7. Cpt1a activity assay

The method quantitating the Cpt1a activity was modified based on previous publications [19–21]. The activity was detected spectrophotometrically by measuring the release of CoA-SH from palmitoyl-CoA at the absorbance of 412 nm using the general thiol reagent 5,5′-dithio-bis-(2-nitrobenzoic acid) (DTNB). Briefly, equal amouts of cellular lysate of various groups was mixed with the DTNB reaction buffer (116 mM Tris, 2.5 mM EDTA, 2 mM DTNB and 0.2% Triton X-100, pH 8.0) and incubated at room temperature for 20 min to eliminate thiol groups. The resulting background absorbance was measured. To start the reaction, the substrates palmitoyl-CoA (final at 100 μM; stock prepared in ddw) and L-carnitine (final at 5 Mm; stock prepared in 1 M Tris, pH 8.0) were added to the reaction mixtures, and immediately subjected to kinetic reading for 1 h. The difference between absorbance readings with and without substrates determined the release of CoA-SH, and readouts were corrected for total protein.

2.8. Statistical analysis

All data were expressed as mean ± SEM. Normal distribution was analyzed to determine whether data met the assumptions of the statistical test. Statistical analyses were performed with either an unpaired student's *t*-test or one-way ANOVA with Tukey's post hoc test, with $p < 0.05$ considered significant.

All other methods, such as dual luciferase reporter assay, real-time quantitative PCR, mitochondrial and nuclei isolation, Ca^{2+} quantification, reactive oxygen species (ROS) detection, hydroxyproline assay, fluorescence assay, ELISA, and ChIP, are described in detail in the supplementary file.

3. Results

3.1. MCU expression and mitochondrial Ca^{2+} are increased in IPF lung macrophages

The primary function of MCU is the uptake of calcium into the mitochondrial matrix. Because MCU regulates the phenotype of macrophages and lung macrophages from IPF subjects have a profibrotic phenotype [16,22], we asked if MCU and Ca^{2+} were increased in IPF. MCU gene expression in lung macrophages was significantly higher in IPF subjects compared to normal subjects (Fig. 1A). Likewise, MCU protein expression was four-fold higher in lung macrophage mitochondria from IPF subjects (Fig. 1B and C). The increased level of MCU correlated with a markedly higher content of Ca^{2+} in the mitochondria of IPF lung macrophages (Fig. 1D).

To confirm that the increase of MCU was limited to lung macrophages, MCU expression was determined in lung tissue. IPF subjects had significantly higher level of MCU in lung macrophages/monocytes, as characterized by expression of F4/80, the major cell surface marker for macrophages (Fig. 1E). In contrast, IPF and normal subjects had a similar amount of MCU in Type II alveolar epithelial cells, as indicated by expression of surfactant protein C (SPC), the membrane marker of the surfactant-producing Type II cells (Fig. 1F). *In vivo,* lung macrophages from bleomycin-injured mice had a time-dependent increase of MCU expression (Fig. 1G). These observations suggest that macrophage MCU may have a critical role in the pathogenesis of pulmonary fibrosis.

To determine if macrophage MCU contributed to bleomycin-induced alveolar epithelial injury to initiate fibrosis development, we performed reciprocal bone marrow (BM) chimera using WT and MCU $^{\pm}$ mice to focus on recruited macrophages from the bone marrow. Recipients of WT BM had parenchymal collagen deposition, regardless of host genotype, whereas recipients of MCU $^{\pm}$ BM had essentially normal lung architecture (Fig. 1H). These histological observations were confirmed biochemically by measuring the major component of collagen, hydroxyproline (Fig. 1I). The predominant cells in bronchoalveolar lavage (BAL) fluid (> 95%) from both WT and MCU $^{\pm}$ mice were monocytic, again, regardless of the recipient genotype (Fig. S1A), suggesting that recruited monocytes/macrophages are key to fibrosis development.

To provide more direct evidence of the importance of macrophage MCU in the pathogenesis of fibrosis, we generated mice harboring a conditional overexpression of *DN-MCU* in macrophages (*DN-MCU-Lyz2-cre*). *DN-MCU* expression was detected in BAL cells by probing for the Myc tag (Fig. S1B); however, *DN-MCU* was not expressed in Type II alveolar epithelial cells (Fig. S1C). Similar to MCU $^{\pm}$ mice, monocytic cells were the predominant cell type in the BAL fluid from the *DN-MCU-Lyz2-cre* mice after bleomycin-induced injury (Fig. S1D). Because the role of MCU is the transport of Ca^{2+} into the mitochondrial matrix, we assessed if this occurred *in vivo* in the fibrosis model. Mitochondrial Ca^{2+} was significantly increased in lung macrophages from bleomycin-injured WT mice and was markedly reduced in *DN-MCU-Lyz2-cre* mice to a concentration lower than seen in WT saline controls (Fig. 1J). A previous study showed that macrophages exposed to chrysotile asbestos had a dramatic increase in cytosolic calcium levels [23]. We found that intracellular calcium was lower in macrophages expressing MCU_{WT}, whereas intracellular calcium was significantly increased by MCU_{DN} expression compared to the empty vector control (Figs. S1E and F). In aggregate, these data suggest that MCU specifically regulates calcium concentration to prevent cytosolic overload in macrophages.

The biological significance of the difference in mitochondrial Ca^{2+} levels between the WT and *DN-MCU-Lyz2-cre* mice was evaluated. α–smooth muscle actin (α-SMA) is considered marker of the differentiation of myofibroblasts, which are the cells responsible for collagen deposition [24,25]. The presence of α-SMA was significantly increased in the lung tissue of bleomycin-injured WT mice, whereas α-SMA expression in *DN-MCU-Lyz2-cre* mice was similar to saline-exposed WT

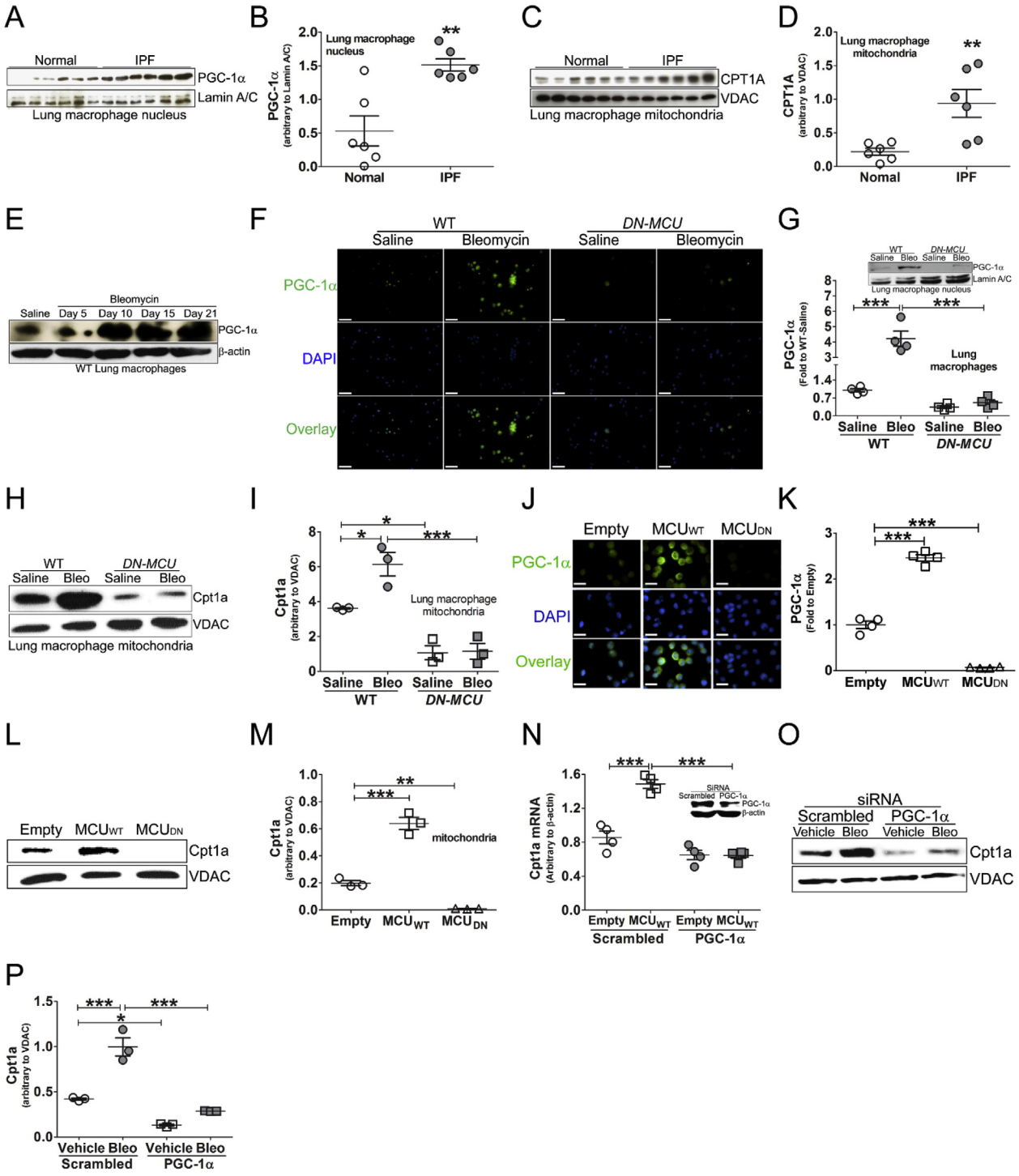

Fig. 2. FAO enzymes in lung macrophages are regulated by MCU.

(A) Immunoblot analysis for PGC-1α in lung macrophage nuclear extracts from human subjects. (B) Statistical analysis, $n = 6$. (C) Immunoblot analysis for CPT1A in lung macrophage mitochondria of human subjects. (D) Statistical analysis, $n = 6$. (E) WT mice were exposed to saline or bleomycin. Lung macrophages were harvested by BAL at indicated time points. Immunoblot analysis of PGC-1α was performed. (F) PGC-1α was determined by fluorescent microcopy in lung macrophages from saline- or bleomycin-exposed WT or *DN-MCU-Lyz2-cre* mice, scale bars, 20 μm. (G) Statistical analysis, $n = 4$ Inset: PGC-1α was detected by immunoblot analysis in isolated nuclear extracts from mice lung macrophages. Lung macrophage mitochondria were isolated from saline- or bleomycin-exposed WT or *DN-MCU-Lyz2-cre* mice, and subjected to (H) immunoblot analysis of Cpt1a. (I) Statistical analysis, $n = 3$. MH-S cells were transfected with empty, MCU_{WT}, or MCU_{DN}. (J) Cells were subjected to fluorescent microscopy for PGC-1α, scale bars, 10 μm. (K) Statistical analysis, $n = 4$. (L) Mitochondria were isolated for immunoblot analysis of Cpt1a. (M) Statistical analysis, $n = 3$. (N) MH-S cells were co-transfected with empty or MCU_{WT} in combination with scrambled or PGC-1α siRNA. Total RNA was isolated for the measurement of Cpt1a mRNA by real-time PCR, $n = 4$. MH-S cells were transfected with scrambled or PGC-1α siRNA, and exposed to vehicle or bleomycin (0.0126 U/ml, 3 h). (O) Immunoblot analysis of Cpt1a in isolated mitochondria. (P) Statistical analysis, $n = 3$. All data are expressed as mean ± SEM. Bleo, bleomycin; DN-MCU, *DN-MCU-Lyz2-cre*. One-way ANOVA with Tukey's post hoc comparison (G, I, K, M, N, and P). Two-tailed student's *t*-test (B and D). $^{*}p \leq 0.05$, $^{**}p \leq 0.01$ and $^{***}p \leq 0.001$. See also Fig. S2.

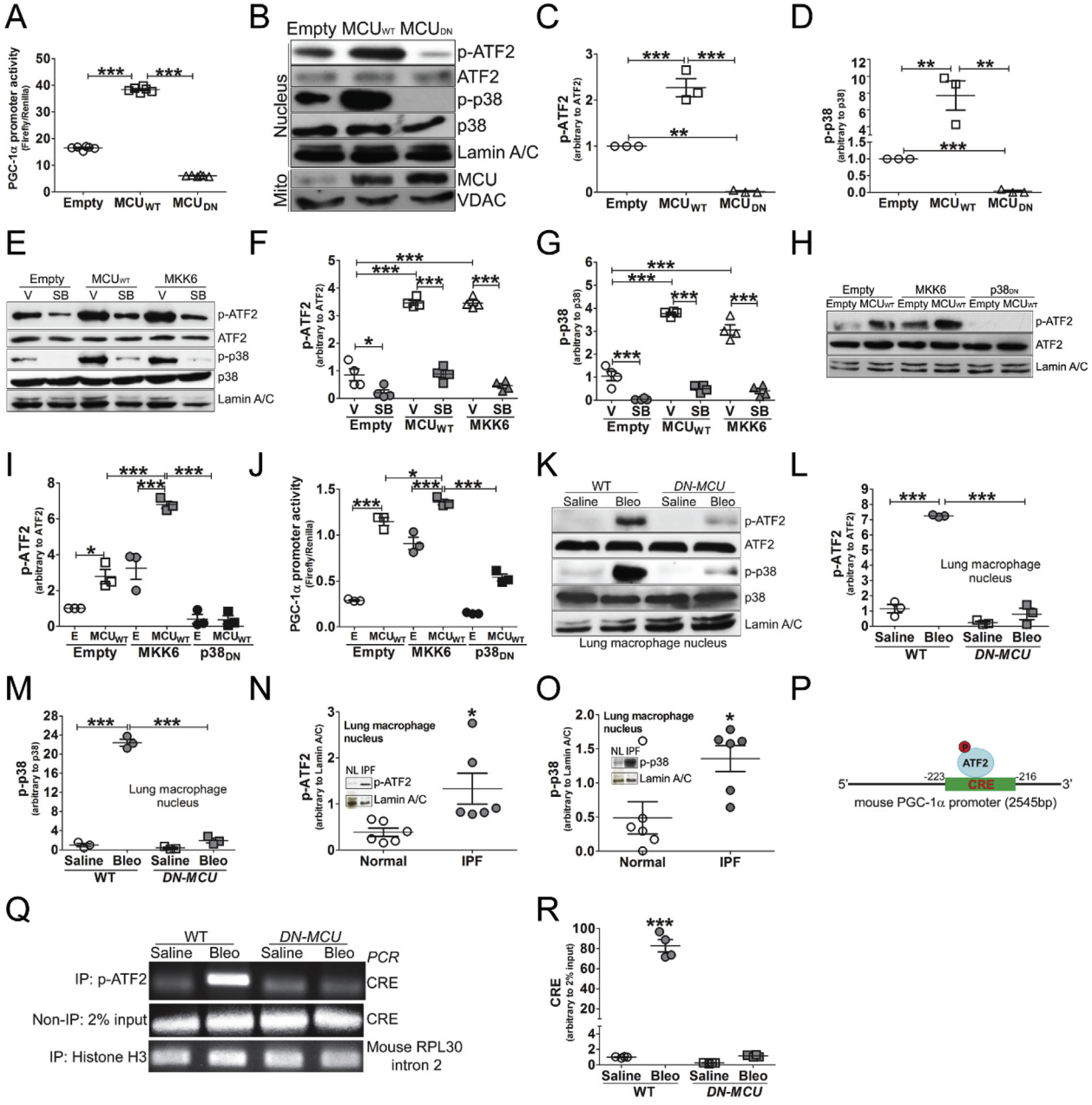

Fig. 3. PGC-1α is transcriptionally activated by MCU.

(A) MH-S cells were co-transfected with renilla luciferase plasmid, pGL3-PGC-1α luciferase promoter combined with empty, $MCU_{WT,}$ or MCU_{DN}. The PGC-1α promoter activity was determined by measuring firefly luciferase and renilla luciferase, and represented with the ratio of firefly to renilla, $n = 6$. MH-S cells were transfected with empty, MCU_{WT}, or MCU_{DN}. (B) Immunoblot analysis was performed for p-ATF2 and p-p38 in nuclear extracts and MCU in isolated mitochondria. (C) Statistical analysis for p-ATF2, $n = 3$. (D) Statistical analysis for p-p38, $n = 3$. (E) MH-S cells were transfected with empty, MCU_{WT}, or $MKK6_{CA}$, and treated with vehicle (V) or SB203580 (SB, 10 μm for 2 h). Immunoblot analysis for p-ATF2 and p-p38 was performed in nuclear extracts. (F) Statistical analysis for p-ATF2, $n = 3$. (G) Statistical analysis for p-p38, $n = 3$. (H) MH-S cells were transfected with empty, MKK6, or $p38_{DN}$ in combination with empty or MCU_{WT}. Immunoblot analysis for p-ATF2 was performed in nuclear extracts. (I) Statistical analysis for p-ATF2, $n = 3$. (J) MH-S cells were transfected with empty, MKK6, or $p38_{DN}$ in combination with empty or MCU_{WT}. Cells were also transfected with renilla luciferase plasmid and pGL3-PGC-1α luciferase promoter. The PGC-1α promoter activity is expressed as the ratio of firefly to renilla, $n = 3$. (K) WT and *DN-MCU-Lyz2-cre* littermates were exposed to saline or bleomycin (1.75U/kg) for 21 days. Lung macrophages were isolated by BAL. Immunoblot analysis for p-ATF2 and p-p38 was performed in nuclear extracts. (L) Statistical analysis for p-ATF2, $n = 3$. (M) Statistical analysis for p-p38, $n = 3$. (N) Statistical analysis of immunoblot analysis for p-ATF2 in lung macrophage nuclear extracts from normal and IPF subjects, $n = 6$. Inset, representative immunoblot analysis. (O) Statistical analysis of immunoblot analysis for p-p38 in lung macrophage nuclear extracts from normal and IPF subjects, $n = 6$. Inset, representative immunoblot analysis. (P) Schematic illustration showing site of p-ATF2 binding to the PGC-1α promoter in the cAMP response element (CRE) domain. WT and *DN-MCU-Lyz2-cre* littermates were exposed to saline or bleomycin (1.75U/kg) for 21 days. Lung macrophages were isolated by BAL and subjected to ChIP analysis of p-ATF2 bound to the PGC-1α promoter DNA by in the CRE domain with (Q) standard PCR or (R) quantitiative PCR, $n = 6$. All data are expressed as mean ± SEM. One-way ANOVA with Tukey's post hoc comparison. Two-tailed student's *t*-test (N and O). $^{*}p \leq 0.05$, $^{**}p \leq 0.01$ and $^{***}p \leq 0.001$. See also Fig. S3.

mice (Fig. 1K and L). The *DN-MCU-Lyz2-cre* mice had normal lung architecture (Fig. 1M). Architectural distortion and collagen deposition were evident in the lungs from the bleomycin-injured WT mice, whereas the *DN-MCU-Lyz2-cre* mice maintained normal lungs without collagen deposition. These findings were validated by hydroxyproline assay (Fig. 1N). Taken together, these observations suggest that the activity of MCU in lung macrophages is critical for the pathogenesis of pulmonary fibrosis.

3.2. Expression of FAO enzymes is regulated by MCU

Because MCU modulates the macrophage phenotype [22], we asked if this regulation was, in part, due to metabolic reprogramming. We first determined if PGC-1α, which increases the enzymatic capacity for FAO, was increased in macrophages from IPF subjects. PGC-1α expression in the nucleus was three-fold higher in lung macrophages from IPF subjects compared to normal subjects (Fig. 2A and B). Likewise, there was a seven-fold higher level of PGC-1α gene expression in lung macrophages of IPF subjects (Fig. S2A). Carnitine palmitoyltransferase 1A (CPT1A), the rate-limiting enzyme for FAO, was increased in lung macrophage mitochondria from IPF subjects (Fig. 2C and D). Conversely, PFKFB3, the key enzyme facilitating glycolysis, was significantly reduced in IPF lung macrophages when compared to normal subjects (Fig. S2B). The observation of increased PGC-1α in IPF subjects was recapitulated *in vivo*, as bleomycin-induced injury triggered an increase in PGC-1α in lung macrophages at 10 days that was maintained through 21 days (Fig. 2E).

To determine if these enzymes were regulated by MCU during fibrotic repair, we analyzed their expression *in vivo*. Bleomycin-injured WT mice had more PGC-1α in the nucleus (Fig. 2F and G) and Cpt1a in mitochondria (Fig. 2H and I) of lung macrophages than the mice exposed to saline. PGC-1α and Cpt1a expression in lung macrophages from *DN-MCU-Lyz2-cre* mice injured with bleomycin was less than the WT saline controls. The reverse was seen for glycolytic enzymes. The lung macrophages from bleomycin-injured WT mice had decreased PFKFB3, whereas the *DN-MCU-Lyz2-cre* mice had increased expression of this glycolytic enzyme (Figs. S2C and D). Moreover, bleomycin-induced injury triggered a rapid decrease of PFKFB3 protein levels that was maintained for 21 days in lung macrophages from WT mice (Fig. S2E). In aggregate, these data suggest that metabolic reprogramming to FAO is a key feature of lung macrophages during fibrotic repair.

The *in vivo* findings were validated genetically *in vitro*. Confocal microscopy analysis showed that MCU_{WT} overexpression promoted PGC-1α localization in nuclei, whereas the dominant negative MCU (MCU_{DN}) significantly diminished PGC-1α nuclear content (Fig. 2J and K). Similar findings were seen with Cpt1a expression in mitochondria (Fig. 2L and M). Silencing MCU with MCU shRNA decreased mitochondrial Cpt1a (Fig. S2F), whereas PFKFB3 was increased by silencing MCU (Fig. S2G) or by overexpression of MCU_{DN} (Fig. S2H).

To determine if mitochondrial Ca^{2+} influx directly regulated expression of FAO enzymes in macrophages, cells were treated with BAPTA-AM to chelate available cytosolic Ca^{2+}. Bleomycin exposure promoted PGC-1α localization in the nucleus and Cpt1a expression in mitochondria; however, chelation of Ca^{2+} by BAPTA-AM decreased the abundance of nuclear PGC-1α and mitochondrial Cpt1a in cells with or without exposure to bleomycin (Figs. S2I and J).

As the key regulator of FAO, PGC-1α regulates Cpt1a expression [26]. To determine if PGC-1α regulated Cpt1a in a MCU-dependent manner in macrophages, we utilized two approaches. First, overexpression of MCU_{WT} increased Cpt1a gene expression in cells transfected with scrambled siRNA, while silencing PGC-1α abolished Cpt1a mRNA levels in cells under all conditions (Fig. 2N). Second, immunoblot analysis demonstrated that silencing PGC-1α decreased mitochondrial Cpt1a content in the presence or absence of bleomycin (Fig. 2O and P). These data suggest that the regulation of macrophage Cpt1a by MCU requires PGC-1α.

3.3. MCU-mediated p38 MAPK activation regulated PGC-1α expression at the transcriptional level

Based on our observation that MCU increased the abundance of nuclear PGC-1α, we investigated the mechanism of this regulation. First, we found that MCU regulated PGC-1α promoter activity, as MCU_{WT} overexpression increased the promoter activity above the empty control, while MCU_{DN} reduced activity below the empty control (Fig. 3A). The molecular mechanism by which MCU regulates PGC-1α promoter activity is not known.

Because MCU induces mitochondrial ROS (mtROS) in multiple cell types [22,27], we evaluated if there was an oxidant-responsive transcriptional element in the PGC-1α promoter. A member of the AP-1 family, ATF2, is known to be induced by oxidative stress and binds to the PGC-1α promoter [28,29]. Since the p38 MAPK activates ATF2 by phosphorylation [30], we asked if MCU regulates PGC-1α by increasing p38 MAPK activation. We found that MCU_{WT} increased ATF2 phosporylation, while MCU_{DN} decreased phosphorylation below the empty control (Fig. 3B and C). The activation of p38 MAPK mirrored the phosphorylation of nuclear ATF2 (Fig. 3B, D). The inhibitory effect of MCU_{DN} on p38 MAPK activiation was confirmed by silencing MCU in macrophages (Fig. S3A, B and C). Macrophages treated with the p38 MAPK inhibitor, SB203580, significantly decreased the phosphorylation of ATF2 by abrogating the activation of p38, even with expression of constitutively active MKK6, the upstream kinase that activates p38 (Fig. 3E, F and G). Furthermore, cells expressing MKK6, MCU_{WT}, or both had increased p-ATF2; however, overexpression of dominant negative p38 ($p38_{DN}$) decreased ATF2 phosphorylation with or without MCU_{WT} overexpression (Fig. 3H and I). The changes in p38 MAPK activation facilitated the activity of the PGC-1α promoter (Fig. 3J). Both MKK6 and MCU_{WT} increased the promoter activity, while $p38_{DN}$ significantly reduced the activity, even in cells expressing MCU_{WT}.

To determine if the phosphorylation of ATF2 and p38 was due to Ca^{2+} signaling, chelating Ca^{2+} with BAPTA-AM significantly decreased the expression p-ATF2 and p-p38 in macrophages in the presence or absence of MCU_{WT} (Fig. S3D, E and F). These findings *in vitro* were recapitulated *in vivo*. Bleomycin-induced injury increased p-ATF2 and p-p38 in the nuclei of lung macrophages from WT mice, while phosphorylation of ATF2 and p38 in *DN-MCU-Lyz2-cre* mice was reduced similar to that seen the WT saline controls (Fig. 3K, L and M). Moreover, these obserations were biologically relevant as there was a significant increase in p-ATF2 (Fig. 3N) and p-p38 (Fig. 3O) in the nuclear extracts from IPF subjects compared to normal subjects.

Because p-ATF2 activates PGC-1α activity by directly binding to the cAMP response element (CRE) domain of the PGC-1α promoter (Fig. 3P), we determined if this occurred *in vivo*. After immunoprecipitation and PCR amplification, the lung macrophages of bleomycin-injured WT mice showed significantly greater p-ATF2 binding to the PGC-1α promoter compared to the *DN-MCU-Lyz2-cre* mice, which was similar to the WT saline controls (Fig. 3Q and R). Taken together, these data suggest that MCU activates the p38 MAPK to increase PGC-1α expression.

3.4. MCU-mediated p38 MAPK activation and FAO enzymes expression were dependent on mitochondrial oxidative stress

Mitochondrial Ca^{2+} is known to mediate mtROS production [22,31,32]. Since MCU-mediated Ca^{2+} signaling was essential in modulating the p38 MAPK, we asked if the regulation of MCU on the p38 MAPK also required mtROS in macrophages. Overexpression of MCU_{WT} increased production of H_2O_2 (Fig. 4A) and superoxide (Fig. S4A) in mitochondria. Silencing the iron-sulfur protein in complex III, Rieske, dramatically decreased the mtROS levels with or without MCU_{WT} overexpression. The decrease in mtROS production by silencing Rieske completely attenuated activiation of the p38 MAPK, as well as the phosphorylation of ATF2 (Fig. 4B, Fig. S4B and C). These data

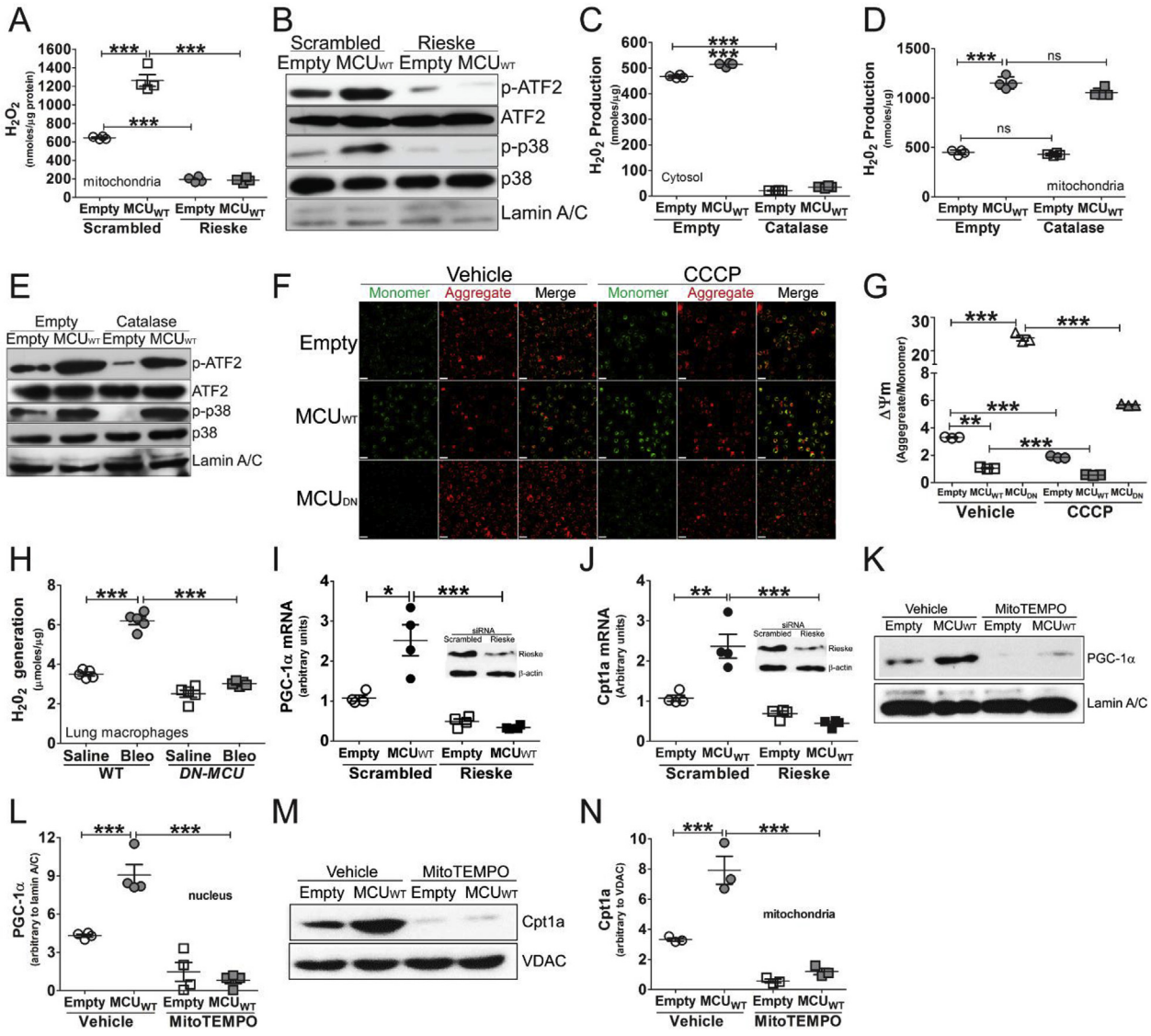

Fig. 4. MCU-mediated p38 MAPK activation and FAO enzymes are dependent on mitochondrial oxidative stress.
THP-1 cells were co-transfected with empty or MCU_{WT} in combination with scrambled or Rieske siRNA. (A) Mitochondria were isolated for the quantitation of H_2O_2 by pHPA assay, $n = 4$; (B) Immunoblot analysis was performed for p-ATF2 and p-p38 in nuclear extracts. THP-1 cells were co-transfected with empty or MCU_{WT} with empty or catalase. Cells were subjected to quantitation of H_2O_2 by pHPA assay (C) in isolated cytosol, $n = 4$ and (D) in mitochondria, $n = 4$. (E) THP-1 cells were co-transfected with empty or MCU_{WT} with empty or catalase. Immunoblot analysis was performed for p-ATF2 and p-p38 in nuclear extracts. (F) THP-1 cells were transfected with empty, MCU_{WT} or MCU_{DN}. Cells were treated with CCCP (3 μM, 30 min) 24 h later. Cells were then labelled with JC-1 (10 μg/ml) for 20 min, and subjected to detection of ΔΨm by confocal imaging. Scale bars, 20 μm. (G) ΔΨm was quantitated by ImageJ and represented as RFU ratio of aggregate/monomer, $n = 3$. (H) WT and *DN-MCU-Lyz2-cre* littermates were exposed to saline or bleomycin for 21 days. Lung macropages were harvested by BAL for quantification of H_2O_2 by pHPA assay in isolated mitochondria, $n = 5$. MH-S cells were transfected with empty or MCU_{WT} in combination of scrambled or Rieske siRNA. Total RNA was extracted to measure (I) PGC-1α mRNA, $n = 4$ and (J) Cpt1a mRNA, $n = 4$. Inset, immunoblot analysis for Rieske. THP-1 cells were transfected with empty or MCU_{WT}, and treated with MitoTEMPO (50 μM, overnight). Cells were subjected to (K) immunoblot analysis for PGC-1α in nuclear extracts. (L) Statistical analysis, $n = 4$; THP-1 cells were transfected and treated as in (K). (M) Immunoblot analysis for Cpt1a in isolated mitochondria. (N) Statistical analysis, $n = 3$. All data are expressed as mean ± SEM. *DN-MCU*, *DN-MCU-Lyz2-cre*. One-way ANOVA with Tukey's post hoc comparison. $^*p \leq 0.05$, $^{**}p \leq 0.01$ and $^{***}p \leq 0.001$. See also Fig. S4.

suggested the importance of mtROS in MCU-mediated p38 MAPK activation.

Prior studies suggest that cytosolic ROS was involved in activating p38 [33,34]. To determine if there was a contribution of cytosolic ROS in addition to mtROS in the MCU-mediated p38 MAPK activation, macrophages expressing catalase, which is located in cytosol of cells (Fig. S4D), markedly decreased cytosolic H_2O_2 levels (Fig. 4C); however, there was no effect on mtROS generation (Fig. 4D and Fig. S4E). Catalase abrogated phosphorylation of ATF2 and p38 in macrophages expressing the empty vector, whereas it had no impact on phosphorylation in the presence of MCU_{WT} (Fig. 4E, Fig. S4F and G). The observations suggest that MCU-mediated p38 MAPK activiation was dependent on mtROS rather than cytosolic ROS.

We have shown that macrophages during fibrosis become dysfunctional and have loss of membrane potential (ΔΨm) [16]. We found that overexpression of MCU_{WT} resulted in loss of ΔΨm when compared to the empty vector control, while MCU_{DN} had a higher ΔΨm than the empty vector (Fig. 4F and G, Fig. S4H). Treating cells with CCCP the day after transfection resulted in greater loss of ΔΨm in cells expressing MCU_{WT}.

It is known that macrophage mitochondrial redox responses, which utilize oxidative phosphorylation, are crucial for pulmonary fibrosis

development [16,22,35]. Because MCU induces mtROS, we asked if mtROS modified the enzymatic capacity for FAO. Lung macrophages from bleomycin-injured WT mice generated high levels of mitochondrial H_2O_2 (Fig. 4H) and superoxide (Fig. S4I), whereas mtROS in the *DN-MCU-Lyz2-cre* mice were similar to the saline control mice. These results indicate that MCU is responsible, at least in part, for generation of mtROS in response to bleomycin injury.

We questioned if MCU-mediated mtROS regulated expression of the enzymes necessary for FAO. MCU_{WT} increased the gene expression of PGC-1α (Fig. 4I) and Cpt1a (Fig. 4J), whereas gene expression was below the empty control by silencing Rieske. MitoTEMPO was used as an alternative to abrogate mtROS. ROS was increased with MCU_{WT} overexpression and was significantly decreased by MitoTEMPO (Fig. S4J). While MCU_{WT} increased nuclear PGC-1α (Fig. 4K and L) and mitochondrial Cpt1a content (Fig. 4M and N), both proteins were barely detectable with MitoTEMPO treatment. Collectively, the above findings suggest that MCU-mediated mtROS is required for the expression of PGC-1α and Cpt1a for metabolic reprogramming to FAO.

Because our data show that MCU-mediated PGC-1α expression required mtROS and studies indicate that PGC-1α suppresses mtROS [36,37], we asked if PGC-1α had an alternative function in lung macrophages in fibrosis. PGC-1α was increased with MCU_{WT} and with PGC-1α overexpression (Fig. S4K). MCU_{WT} increased mtROS, and overexpression of PGC-1α increased mtROS to a similar level (Fig. S4L). PGC-1α overexpression in macrophages expressing MCU_{WT} had a further increase in mtROS indicating that PGC-1α does not attenuate MCU-mediated mtROS.

3.5. Metabolic reprogramming to FAO is regulated by MCU

Based on our data showed the role of MCU in regulating FAO enzymes, we anticipated that MCU reprograms lung macrophages to FAO during fibrotic repair. We analyzed mitochondrial respiration by measuring oxygen consumtion rate (OCR) in the chimeric mouse model. Mice that received WT BM had a significant increase in OCR in lung macrophages in response to bleomycin injury (Fig. 5A and B). In contrast, mice that received MCU $^{\pm}$ BM had a significant reduction of OCR to the level of the WT saline controls. More direct evidence that MCU regulates lung macrophage mitochondrial respiration was demonstrated with *DN-MCU-Lyz2-cre* mice. Lung macrophages from bleomycin-injured WT mice had a marked increase in mitochondrial respiration, whereas OCR in lung macrophages from *DN-MCU-Lyz2-cre* mice was less than the WT mice exposed to saline (Fig. 5C and D).

To directly demonstrate that FAO was responsible for the increase in OCR, we used palmitate as a substrate. Palmitate increased OCR in the saline controls to the level seen with bleomycin and BSA, while OCR was significantly augmented by the addition of palmitate in lung macrophages from bleomycin-injured WT mice (Fig. 5E). OCR in the macrophages from *DN-MCU-Lyz2-cre* mice was below the BSA WT saline controls, and bleomycin and palmitate had no effect. Similar findings were seen *in vitro*. Overexpression of MCU_{WT} increased OCR that was further enhanced by the addition of palmitate (Fig. 5F and G). OCR in cells expressing MCU_{DN} was below the BSA control, and the addition of palmitate had no effect.

The role of MCU on glycolytic metabolism had the opposite effect. MCU_{WT} reduced the extracellular acidification rate (ECAR), a measure of glycolysis, compared to empty vector, while cells expressing MCU_{DN} had a significantly elevated ECAR compared to MCU_{WT} (Fig. 5H). To show the regulation of PGC-1α on macrophage FAO, cells were transfected with empty or MCU_{WT} in combination with empty or PGC-1α. In cells expressing PGC-1α alone, FAO was increased to the level seen with MCU_{WT} (Fig. 5I). FAO was further elevated in macrophages expressing PGC-1α and MCU_{WT} together.

Sustained mitochondrial Ca^{2+} loading leads to NADH production, which is used by the electron transport chain to generate mitochondrial ATP [38]. Macrophages transfected with MCU_{WT} reduced the ratio of NAD/NADH, whereas cells expressing MCU_{DN} increased the ratio of NAD/NADH (Fig. S5A). The utilization of FAO as an energy source provides more ATP than aerobic glycolysis [39–41]. We found that MCU_{WT}, PGC-1α, and their combination not only increased FAO, but also resulted in a substantial increase in mitochondrial ATP production (Fig. S5B), suggesting an inherent relationship between FAO and bioenergetics. These data suggest that MCU is a crucial regulator for mitochondrial bioenergetics in lung macrophages.

The increase in FAO by MCU_{WT} could be abrogated by etomoxir, the Cpt1a inhibitor (Fig. 5J); however, the trimeric structure of Cpt1a is required for its activity in forming the channel for the transport of fatty acids into mitochondria [42]. Cpt1a activity can be inhibited by the disruption of its trimeric structure by the allosteric inbhitior, malonyl-CoA. Overexpression of MCU_{WT} increased Cpt1a activity, and MCU_{DN} decreased the activity significantly below the empty control (Fig. 5K). Treatment with malonyl-CoA significantly reduced the Cpt1a activity in the presence or absence of MCU_{WT} (Fig. 5L). Acetyl-CoA carboxylase 2 (ACC2) poses an inhibitory function on FAO by targeting Cpt1a via production of malonyl-CoA. Phosphorylation of ACC2 blocks its enzymatic capacity, which renders Cpt1a active [43,44]. Macrophages expressing MCU_{WT} had increased phosphorylation of ACC2 (p-ACC2) in mitochondria, whereas the MCU_{DN} reduced p-ACC2 below the empty control (Fig. 5M and N). The regulation of p-ACC2 by MCU was further confirmed with MCU shRNA (Figs. S5C and D). The importance of the trimeric structure of Cpt1a for FAO was confirmed as malonyl-CoA significantly decreased MCU-mediated FAO below the BSA empty control (Fig. 5O).

To more directly illustrate the effect of mtROS on macrophage FAO, OCR was measured using palmitate as the substrate. FAO was significantly reduced by MitoTEMPO (Fig. S5E). These data demonstrate that MCU is an essential regulator of metabolic reprogramming to FAO in macrophages.

3.6. Metabolic reprogramming and the macrophage phenotype are interdependent

To determine if the phenotype of recruited monocytes/macrophages was modulated by metabolic reprogramming, we generated reciprocal BM chimeras using WT and MCU $^{\pm}$ mice. Bleomycin-injured recipients of WT BM had a dramatic increase in CD206 expression (mannose receptor), a profibrotic surface marker in macrophages, regardless of the host genotype (Fig. 6A and B). Similar observations were seen with MARCO (macrophage receptor with collagenous structure) expression, another profibrotic marker in macrophages (Fig. 6A, C). In contrast, recipients of the MCU $^{\pm}$ BM exposed to saline or bleomycin were similar to the WT saline controls, again, regardless of the host genotype.

To evaluate MCU in a more specific manner, BAL fluid from bleomycin-injured WT mice had a significant increase in active TGF-β1 (Fig. 6D) and PDGF-B (Fig. 6E), whereas concentrations of these factors were significantly reduced in *DN-MCU-Lyz2-cre* mice. The reverse was seen with antifibrotic markers. TNF-α was significantly decreased in BALF from bleomycin-injured WT mice, while it was markedly increased in the BALF from *DN-MCU-Lyz2-cre* mice (Fig. 6F). The above data implicate that MCU-mediated metabolic reprogramming promotes the recruited monocyte/macrophages to polarize to an alternative, profibrotic phenotype after bleomycin injury.

We used a genetic approach to show the relevance of metabolic reprogramming to FAO in modulating the macrophage phenotype. Because TGF-β1 in BAL fluid is primarily derived from macrophages [16], we determined the effect of PGC-1α on regulating TGF-β1 expression. Macrophages exposed to bleomycin had a 3-fold increase in TGF-β1 mRNA, whereas silencing PGC-1α reduced gene expression to control levels regardless of bleomycin exposure (Fig. 6G). Active TGF-β1 in conditioned media was significantly attenuated by silencing Cpt1a (Fig. 6H). In contrast, TNF-α gene expression and protein levels in BAL fluid were increased with silencing PGC-1α (Fig. 6I) or Cpt1a

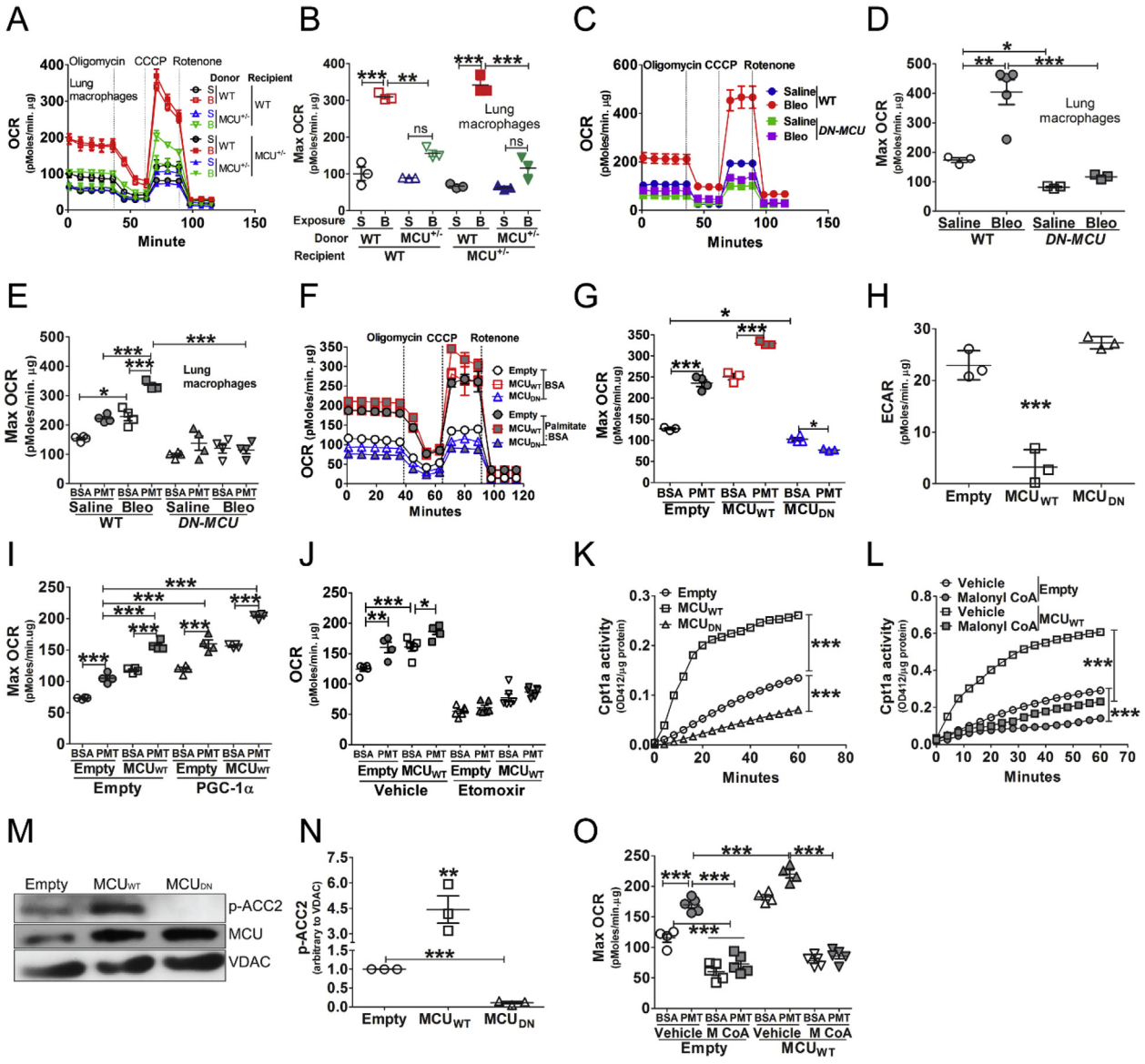

Fig. 5. MCU regulates metabolic reprogramming to FAO in macrophages.
Reciprocal bone marrow chimeric mice were exposed to saline or bleomycin. Lung macrophages from were harvested by BAL. (A) OCR kinetics and (B) Max OCR are shown, $n = 3$. (C) WT and *DN-MCU-Lyz2-cre* littermates were exposed to saline or bleomycin for 21 days. Lung macrophages were harvested for the determination of OCR, $n = 3$ or 5. (D) Max OCR, $n = 3$ or 5. (E) WT and *DN-MCU-Lyz2-cre* littermates were exposed to saline or bleomycin for 21 days. Lung macropages were harvested by BAL. FAO was determined by measuring OCR with palmitate as substrate. Results are shown as max OCR, $n = 4$. MH-S cells were transfected with empty, MCU_{WT}, or MCU_{DN}. (F) Kinetics of OCR using palmitate as a substrate. (G) Max OCR, $n = 3$ or 4. (H) MH-S cells were transfected with empty, MCU_{WT}, or MCU_{DN}. Cells were subjected to seahorse assay to obtain ECAR, $n = 4$. (I) MH-S cells were transfected with empty or MCU_{WT}, in combination with empty or PGC-1α. FAO was determined by OCR using palmitate as a substrate. Max OCR, $n = 4$. (J) MH-S cells were transfected with empty or MCU_{WT}, and treated with etomoxir (40 μM) overnight. Cells were subjected to FAO by OCR measurement, $n = 4$–6. (K) MH-S cells were transfected with empty, MCU_{WT}, or MCU_{DN} and whole lysate was prepared for the determination of Cpt1a activity, $n = 4$. (L) MH-S cells were transfected with empty or MCU_{WT}, and treated with vehicle or malonyl CoA (100 μm, 3 h). Whole lysate was prepared for the determination of Cpt1a activity, $n = 4$. (M) MH-S cells were transfected with empty, MCU_{WT}, or MCU_{DN}. Immunoblot analysis for p-ACC2 in isolated mitochondria. (N) Statistical analysis, $n = 3$. (O) MH-S cells were transfected with empty or MCU_{WT} and treated with vehicle or malonyl CoA. FAO was determined by OCR using palmitate as a substrate, $n = 4$–5. All average data were represented as mean ± SEM. S, saline; B and Bleo, bleomycin; PMT, palmitate; DN-MCU, *DN-MCU-Lyz2-cre*. One-way ANOVA with Tukey's post hoc comparison. $^{*}p \leq 0.05$, $^{**}p \leq 0.01$ and $^{***}p \leq 0.001$. See also Fig. S5.

(Fig. 6J), suggesting that inhibition of FAO induces macrophages to activate in a classical fashion.

To determine if MCU-mediated alternative activation of macrophages required FAO, Cpt1a was silenced in cells expressing MCU_{WT}. Overexpression of MCU_{WT} markedly increased CD206 five-fold compared to the empty control (Fig. 6K and L). Silencing Cpt1a decreased CD206 expression below the empty controls regardless of MCU_{WT} overexpression. Similar observations were seen with expression of MARCO (Fig. 6K, M).

Because our data indicate that the profibrotic phenotype was abrogated by silencing PGC-1α, we questioned if FAO was attenuated in mice harboring a deletion of TGF-β1 (*Tgfb1*$^{-/-}$*Lyz2-cre*) in macrophages (Fig. 6N). Lung macrophages from *Tgfb1*$^{-/-}$*Lyz2-cre* mice do not polarize to a profibrotic phenotype, and these mice are protected from pulmonary fibrosis after bleomycin injury [16]. PGC-1α was increased in lung macrophages from bleomycin-injured WT mice, whereas PGC-1α was absent in the macrophages from *Tgfb1*$^{-/-}$*Lyz2-cre* mice (Fig. 6N and O). Similar results were observed in PGC-1α gene

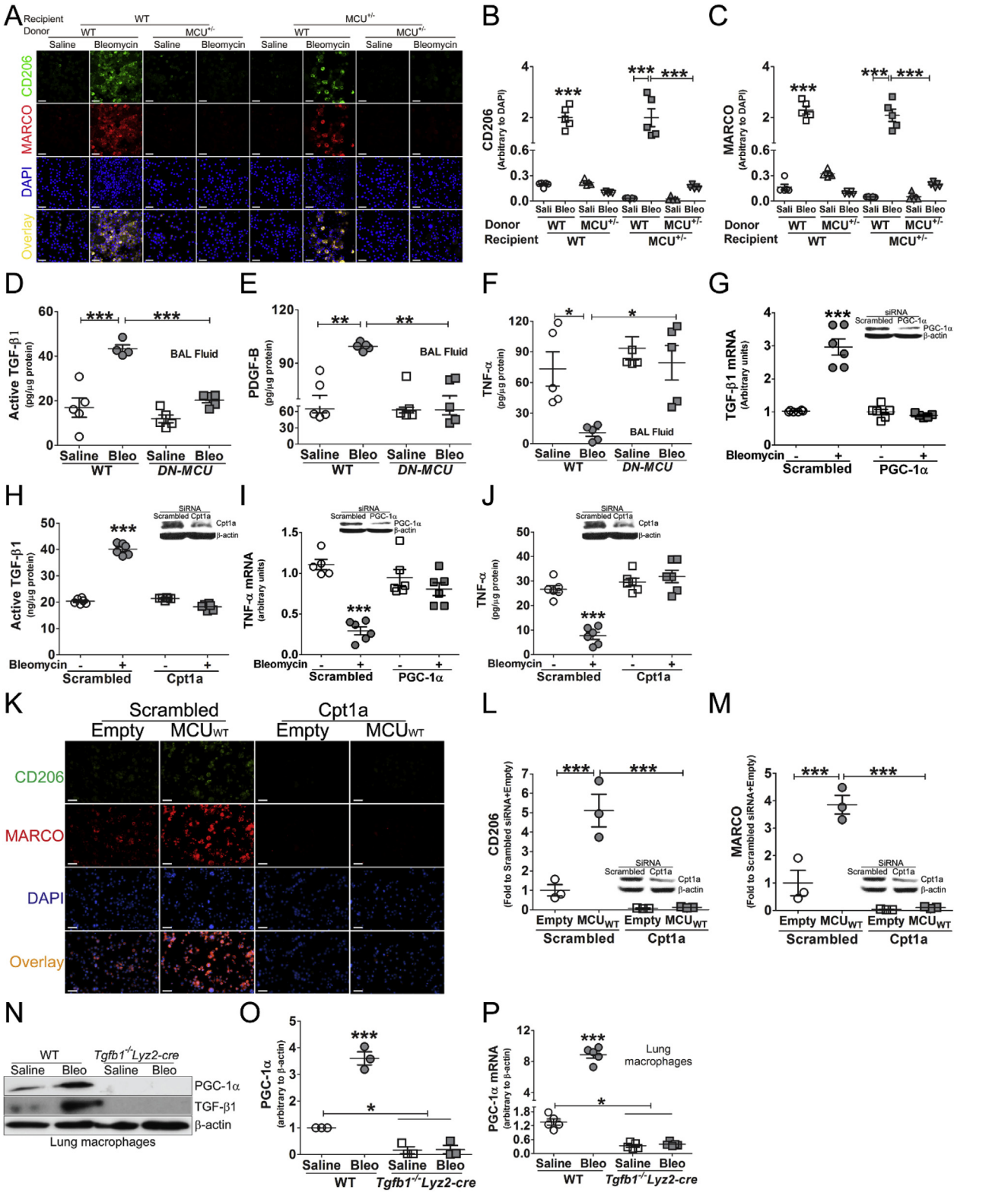

(caption on next page)

expression (Fig. 6P). These results indicate there is an interdependence between the profibrotic phenotype and FAO in lung macrophages during fibrosis. In aggregate, these observations strongly suggest that metabolic reprogramming to FAO in lung macrophages has a critical role in the pathogenesis of pulmonary fibrosis. Moreover, these observations indicate that MCU is a novel therapeutic target to halt fibrotic repair.

4. Discussion

Metabolic homeostasis is important for cells, tissues, and organs to maintain a normal physiological status. Metabolic reprogramming, however, is often associated with disease pathogenesis or progression. Metabolic reprogramming that entails FAO and oxidative phosphorylation is a key feature of macrophages during repair of injured tissue

Fig. 6. Metabolic reprogramming and macrophage phenotype are interdependent.
(A) Lung macrophages from bone marrow chimeric mice were harvested to measure CD206 and MARCO by confocal analyses, scale bars, 20 μm. Statistical analyses of (B) CD206 and (C) MARCO were performed, $n = 5$. BAL fluid was harvested from WT and *DN-MCU-Lyz2-cre* mice for the determination of (D) active TGF-β1, $n = 5$, (E) PDGF-B, $n = 5$, and (F) TNF-α by ELISA, $n = 5$. (G) MH-S cells were transfected with scrambled or PGC-1α siRNA and exposed to bleomycin (0.0126 U/ml, 4 h). Total RNA was isolated for the quantitation of TGF-β1 mRNA by real-time quantitative PCR, $n = 5$. (H) MH-S cells were transfected with scrambled or Cpt1a siRNA and exposed to bleomycin (0.0126 U/ml, overnight). Conditioned media were collected for the detection of active TGF-β1 by ELISA, $n = 6$. (I) MH-S cells were transfected to with scrambled or PGC-1α siRNA. Cells were exposed to bleomycin (0.0126 U/ml, 4 h). Total RNA was isolated for the measurement of TNF-α mRNA by real-time PCR, $n = 5$. (J) MH-S cells were transfected with scrambled or Cpt1a siRNA. Cells were exposed to bleomycin (0.0126 U/ml, overnight). Conditioned media were collected for the measurement of TNF-α by ELISA, $n = 6$. (K) MH-S cells were co-transfected with empty or MCU_{WT} in combination of scrambled or Cpt1a siRNA. Cells were then subjected fluorescent microscopy for CD206 and MARCO; scale bars, 20 μm; Statistical analyses for (L) CD206, $n = 3$ and (M) MARCO, $n = 3$. (N) WT and *Tgfb1*$^{-/-}$*Lyz2-cre* mice were exposed to saline or bleomycin (1.75U/kg) for 21 days. Lung macrophages were harvested by BAL for the detection of PGC-1α by immunoblot analysis. (O) Statistical analysis, $n = 3$. (P) Total RNA was isolated from lung macrophages of *Tgfb1*$^{-/-}$*Lyz2-cre* mice and WT mice for the measurement of PGC-1α gene expression level by qRT-PCR, $n = 5$. All data are expressed as mean ± SEM. Sali, Saline; Bleo, Bleomycin; *DN-MCU*, *DN-MCU-Lyz2-cre*. One-way ANOVA with Tukey's post hoc comparison. *$p \leq 0.05$, **$p \leq 0.01$ and ***$p \leq 0.001$.

[39,40]. The reprogramming in these macrophages is necessary to support long-term cellular activities, such as lung remodeling, as well as an increase in the apoptotic resistance that is seen in these cells [41,45]. In the current study, metabolic reprogramming shifted glycolysis to FAO in macrophages from bleomycin-injured mice. The rationale of investigating metabolic reprogramming in the pathogenesis of disease is to develop efficacious and potent therapeutic agents to halt fibrosis progression.

Metabolic reprogramming has an important role in multiple diseases. For example, in cardiac hypertrophy and breast cancer, cells undergo metabolic reprogramming from FAO to aerobic glycolysis [46–48]. After chemotherapy breast cancer cells reprogram to FAO, which is associated with an increased recurrence; however, pharmacologic inhibition of FAO by etomoxir decreased bioenergetics to abrogate the extent of recurrence of breast cancer [49,50]. Liver fibrosis can develop from the excess deposition of triglycerides in hepatocytes. This storage occurs due to a defect in FAO via impairment or inhibition of PPAR [51,52]. In contrast to our data, metabolic reprogramming to FAO in tubular epithelial cells protects against kidney fibrosis in end-stage renal disease [53].

Studies indicate the role of MCU in metabolism is to regulate glycolysis. In hyperglycemia, MCU expression is reduced, which was associated with upregulated FAO, whereas overexpression of MCU reprogrammed cardiac myocytes to utilize glucose oxidation for energy [13]. In pancreatitic β-cells, the MCU-mediated increase in mitochondrial Ca^{2+} was required for glucose-induced ATP production for insulin release [54]. Furthermore, MCU regulates the expression of HIF-1α, which mediates the Warburg effect, or aerobic glycolysis, in breast cancer cells and other cancers [11,55]. Our observations in lung macrophages contrasts the experimental finding in cardiac myocytes, pancreatic β-cells, and cancer in that MCU decreased enzymes involved in glycolysis and increased proteins necessary for FAO. This may be due to differences in cell type or disease specificity.

The molecular basis of PGC-1α gene expression is dependent, in part, on specific transcription factors. PGC-1α expression in skeletal muscle during exercise is dependent on activation of ATF2, a transcription factor of the AP-1 family [29]. ATF2 activation requires phosphorylation by a serine/threonine-specific kinase, one of which is the p38 MAPK. MCU-mediated mtROS has not been linked to p38 or ATF2 previously. Although an inhibitor of p38 attenuates bleomycin-induced fibrosis in mice [56], the mechanism by which this occurs is not known. The p38 MAPK is critical for PGC-1α activation as it regulates expression transcriptionally, as our data demonstrates, and post-translationally by phosphorylation at specific residues [57]. Although transcription factors other than ATF2 are likely necessary for PGC-1α expression, our observations suggest a unique role for MCU in lung macrophages by regulating metabolic reprogramming via activation of the p38 MAPK and phosphorylation of ATF2, which increases expression and activation of PGC-1α.

The association of ROS with metabolic reprogramming is somewhat controversial. ROS is known to increase PGC-1α gene expression [58]; however, PGC-1α, a transcriptional proponent of oxidative phosphorylation, is a key regulator of mtROS production and mitochondrial function. Studies indicate that PGC-1α suppresses mtROS production by increasing expression of antioxidant enzymes [36,37], suggesting that inhibition of mtROS is necessary to promote FAO. In contrast, we found that PGC-1α does not attenuate MCU-mediated mtROS, which is a paradigm shift compared to other studies investigating PGC-1α-mediated metabolic reprogramming to FAO.

The effect of ROS on metabolic reprogramming has been linked to glucose levels. Specifically, ROS represses FAO when glucose levels are normal, while induction of FAO occurs in cells when glucose is low [59]. PGC-1α expression and activity is increased by ROS to mediate FAO in hepatitis C, but it is not clear if the ROS production is maintained in the infected cells [60]. Interestingly, the reverse also occurs in that FAO results in increased mtROS production in the kidney [61]. To our knowledge, there are no investigations regarding metabolic reprogramming in IPF lung macrophages, but mtROS production, which is dependent on mitochondrial Ca^{2+} influx in macrophages, is known to have an important role in the pathogenesis of fibrosis [16,62,63]. Here, our observations show a critical relationship between mitochondrial Ca^{2+}, mtROS, PGC-1α activity, and metabolic reprogramming to FAO that contributes to the pathogenesis of lung fibrosis.

The reliance on FAO by alternatively activated macrophages and aerobic glycolysis by classically activated macrophages is well-known [40]. Aerobic glycolysis provides macrophages with ATP and metabolites to perform functions over short time periods. In contrast, FAO and oxidative phosphorylation in alternatively activated macrophages affords them to be involved in long-term cellular activities and cellular permanence, as seen in prolonged wound healing [39,41]. Moreover, the efficiency of FAO is more effective than glycolysis in meeting the bioenergetics required for their long-term roles. Inhibition of FAO and oxidative phosphorylation enhances the expression of glycolytic metabolites to induce classical activation. Our observations support this notion as inhibition of MCU increased PFKFB3 and ECAR, whereas MCU expression increased FAO *in vitro* and *in vivo*. A recent study showed that profibrotic macrophages utilized glycolytic metabolism [64]; however, evaluation of glycolysis and FAO was done at 14 days after bleomycin, which may represent acute lung injury rather than fibrosis. In addition, fibrotic remodeling was not shown in that study, so it is unclear if the effect of glycolysis was associated with pro-inflammatory markers, which are present during acute lung injury. In contrast, our data indicate an interdependence in profibrotic polarization and FAO. Our prior data show that lung macrophages in pulmonary fibrosis display alternative activation [16,22,35,62], and our current observations reveal a distinctive role for MCU in metabolic reprogramming to FAO to promote progression of fibrotic repair.

In aggregate, this study demonstrated that MCU-mediated metabolic reprogramming to FAO in lung macrophages was regulated by increasing mtROS to induce transcriptional activation of PGC-1α via activation of the p38 MAPK. Moreover, expression of dominant-negative MCU in macrophages protected mice from fibrosis development via

metabolic reversal to glycolysis. Moreover, this study indicates that there is an interdependence of MCU-mediated metabolic reprogramming to FAO and profibrotic polarization of lung macrophages. These observations suggest that MCU and mitochondrial Ca^{2+} influx are novel therapeutic targets to halt pulmomary fibrosis.

Author contributions

L. Gu and A. B. Carter developed the hypothesis and designed the experiments; L. Gu, J. L. Larson-Casey, J. H. Lee, and S. Meza-Perez performed the experiments; L. Gu, J. L. Larson-Casey, T. D. Randall, S. A. Andrabi, and A. B. Carter analyzed the data; and L. Gu and A. B. Carter wrote the manuscript.

Conflict of interest

The authors declare no competing interests.

Acknowledgments

This work was supported, in whole or in part, by the U.S. National Institutes of Health (NIH) grants ES015981-12 and ES027464-01 and Department of Veteran Affairs grant I01 CX001715-01 (to ABC). Additional support was provided by R01-NS08695301 (to SAA) and Pulmonary Fibrosis Foundation (Award number 2019650 to LG).

Appendix A. Supplementary data

Supplementary data to this article can be found online at https://doi.org/10.1016/j.redox.2019.101307.

References

[1] G. Raghu, D. Weycker, J. Edelsberg, W.Z. Bradford, G. Oster, Incidence and prevalence of idiopathic pulmonary fibrosis, Am. J. Respir. Crit. Care Med. 174 (2006) 810–816.
[2] A.S. Lee, I. Mira-Avendano, J.H. Ryu, C.E. Daniels, The burden of idiopathic pulmonary fibrosis: an unmet public health need, Respir. Med. 108 (2014) 955–967.
[3] J. Gribbin, R.B. Hubbard, I. Le Jeune, C.J. Smith, J. West, L.J. Tata, Incidence and mortality of idiopathic pulmonary fibrosis and sarcoidosis in the UK, Thorax 61 (2006) 980–985.
[4] Helen E. Jo, Ian Glaspole, Christopher Grainge, Nicole Goh, M. Peter, A. Hopkins, Yuben Moodley, Paul N. Reynolds, Sally Chapman, E. Haydn Walters, Christopher Zappala, Heather Allan, Gregory J. Keir, Andrew Hayen, Wendy A. Cooper, Annabelle M. Mahar, Samantha Ellis, Sacha Macansh, J. Tamera, Baseline characteristics of idiopathic pulmonary fibrosis: analysis from the Australian Idiopathic Pulmonary Fibrosis Registry, Corte. Eur Respir J 49 (2017) 1651592. Eur Respir J 2017; 49.
[5] J. Hutchinson, A. Fogarty, R. Hubbard, T. McKeever, Global incidence and mortality of idiopathic pulmonary fibrosis: a systematic review, Eur. Respir. J. 46 (2015) 795–806.
[6] T.E. King Jr., W.Z. Bradford, S. Castro-Bernardini, E.A. Fagan, I. Glaspole, M.K. Glassberg, E. Gorina, P.M. Hopkins, D. Kardatzke, L. Lancaster, D.J. Lederer, S.D. Nathan, C.A. Pereira, S.A. Sahn, R. Sussman, J.J. Swigris, P.W. Noble, A.S. Group, A phase 3 trial of pirfenidone in patients with idiopathic pulmonary fibrosis, N. Engl. J. Med. 370 (2014) 2083–2092.
[7] L. Richeldi, R.M. du Bois, G. Raghu, A. Azuma, K.K. Brown, U. Costabel, V. Cottin, K.R. Flaherty, D.M. Hansell, Y. Inoue, D.S. Kim, M. Kolb, A.G. Nicholson, P.W. Noble, M. Selman, H. Taniguchi, M. Brun, F. Le Maulf, M. Girard, S. Stowasser, R. Schlenker-Herceg, B. Disse, H.R. Collard, I.T. Investigators, Efficacy and safety of nintedanib in idiopathic pulmonary fibrosis, N. Engl. J. Med. 370 (2014) 2071–2082.
[8] Y. Wu, T.P. Rasmussen, O.M. Koval, M.L. Joiner, D.D. Hall, B. Chen, E.D. Luczak, Q. Wang, A.G. Rokita, X.H. Wehrens, L.S. Song, M.E. Anderson, The mitochondrial uniporter controls fight or flight heart rate increases, Nat. Commun. 6 (2015) 6081.
[9] C. Mammucari, G. Gherardi, I. Zamparo, A. Raffaello, S. Boncompagni, F. Chemello, S. Cagnin, A. Braga, S. Zanin, G. Pallafacchina, L. Zentilin, M. Sandri, D. De Stefani, F. Protasi, G. Lanfranchi, R. Rizzuto, The mitochondrial calcium uniporter controls skeletal muscle trophism in vivo, Cell Rep. 10 (2015) 1269–1279.
[10] H. Yan, D. Zhang, S. Hao, K. Li, C.H. Hang, Role of mitochondrial calcium uniporter in early brain injury after experimental subarachnoid hemorrhage, Mol. Neurobiol. 52 (2015) 1637–1647.
[11] A. Tosatto, R. Sommaggio, C. Kummerow, R.B. Bentham, T.S. Blacker, T. Berecz, M.R. Duchen, A. Rosato, I. Bogeski, G. Szabadkai, R. Rizzuto, C. Mammucari, The mitochondrial calcium uniporter regulates breast cancer progression via HIF-1alpha, EMBO Mol. Med. 8 (2016) 569–585.
[12] L.E. Wright, D. Vecellio Reane, G. Milan, A. Terrin, G. di Bello, A. Belligoli, M. Sanna, M. Foletto, F. Favaretto, A. Raffaello, C. Mammucari, D. Nitti, R. Vettor, R. Rizzuto, Increased mitochondrial calcium uniporter in adipocytes underlies mitochondrial alterations associated with insulin resistance, Am. J. Physiol. Endocrinol. Metab. 313 (2017) E641–E650 ajpendo 00143 02016.
[13] J. Diaz-Juarez, J. Suarez, F. Cividini, B.T. Scott, T. Diemer, A. Dai, W.H. Dillmann, Expression of the mitochondrial calcium uniporter in cardiac myocytes improves impaired mitochondrial calcium handling and metabolism in simulated hyperglycemia, Am. J. Physiol. Cell Physiol. 311 (2016) C1005–C1013.
[14] X. Pan, J. Liu, T. Nguyen, C. Liu, J. Sun, Y. Teng, M.M. Fergusson, Rovira II, M. Allen, D.A. Springer, A.M. Aponte, M. Gucek, R.S. Balaban, E. Murphy, T. Finkel, The physiological role of mitochondrial calcium revealed by mice lacking the mitochondrial calcium uniporter, Nat. Cell Biol. 15 (2013) 1464–1472.
[15] D.D. Hall, Y. Wu, F.E. Domann, D.R. Spitz, M.E. Anderson, Mitochondrial calcium uniporter activity is dispensable for MDA-MB-231 breast carcinoma cell survival, PLoS One 9 (2014) e96866.
[16] J.L. Larson Casey, J.S. Deshane, A.J. Ryan, V.J. Thannickal, A.B. Carter, Macrophage Akt1 kinase-mediated mitophagy modulates apoptosis resistance and pulmonary fibrosis, Immunity 44 (2016) 582–596.
[17] J. Raingeaud, S. Gupta, J.S. Rogers, M. Dickens, J. Han, R.J. Ulevitch, R.J. Davis, Pro-inflammatory cytokines and environmental stress cause p38 mitogen-activated protein kinase activation by dual phosphorylation on tyrosine and threonine, J. Biol. Chem. 270 (1995) 7420–7426.
[18] J. Raingeaud, A.J. Whitmarsh, T. Barrett, B. Derijard, R.J. Davis, MKK3- and MKK6-regulated gene expression is mediated by the p38 mitogen-activated protein kinase signal transduction pathway, Mol. Cell. Biol. 16 (1996) 1247–1255.
[19] E.S. Shin, S.Y. Cho, E.H. Lee, S.J. Lee, I.S. Chang, T.R. Lee, Positive regulation of hepatic carnitine palmitoyl transferase 1A (CPT1A) activities by soy isoflavones and L-carnitine, Eur. J. Nutr. 45 (2006) 159–164.
[20] H. Karlic, S. Lohninger, T. Koeck, A. Lohninger, Dietary l-carnitine stimulates carnitine acyltransferases in the liver of aged rats, J. Histochem. Cytochem. 50 (2002) 205–212.
[21] K. Linher-Melville, S. Zantinge, T. Sanli, H. Gerstein, T. Tsakiridis, G. Singh, Establishing a relationship between prolactin and altered fatty acid beta-oxidation via carnitine palmitoyl transferase 1 in breast cancer cells, BMC Canc. 11 (2011) 56.
[22] L. Gu, J.L. Larson Casey, A.B. Carter, Macrophages utilize the mitochondrial calcium uniporter for profibrotic polarization, FASEB J. 31 (2017) 3072–3083.
[23] A.J. Ryan, J.L. Larson Casey, C. He, S. Murthy, A.B. Carter, Asbestos-induced disruption of calcium homeostasis induces endoplasmic reticulum stress in macrophages, J. Biol. Chem. 289 (2014) 33391–33403.
[24] A. Datta, C.J. Scotton, R.C. Chambers, Novel therapeutic approaches for pulmonary fibrosis, Br. J. Pharmacol. 163 (2011) 141–172.
[25] J.R. Rock, C.E. Barkauskas, M.J. Cronce, Y. Xue, J.R. Harris, J. Liang, P.W. Noble, B.L. Hogan, Multiple stromal populations contribute to pulmonary fibrosis without evidence for epithelial to mesenchymal transition, Proc. Natl. Acad. Sci. U. S. A. 108 (2011) E1475–E1483.
[26] Y. Zhang, K. Ma, S. Song, M.B. Elam, G.A. Cook, E.A. Park, Peroxisomal proliferator-activated receptor-gamma coactivator-1 alpha (PGC-1 alpha) enhances the thyroid hormone induction of carnitine palmitoyltransferase I (CPT-I alpha), J. Biol. Chem. 279 (2004) 53963–53971.
[27] T.P. Rasmussen, Y. Wu, M.L. Joiner, O.M. Koval, N.R. Wilson, E.D. Luczak, Q. Wang, B. Chen, Z. Gao, Z. Zhu, B.A. Wagner, J. Soto, M.L. McCormick, W. Kutschke, R.M. Weiss, L. Yu, R.L. Boudreau, E.D. Abel, F. Zhan, D.R. Spitz, G.R. Buettner, L.S. Song, L.V. Zingman, M.E. Anderson, Inhibition of MCU forces extra mitochondrial adaptations governing physiological and pathological stress responses in heart, Proc. Natl. Acad. Sci. U. S. A. 112 (2015) 9129–9134.
[28] A. Bhoumik, S. Takahashi, W. Breitweiser, Y. Shiloh, N. Jones, Z. Ronai, ATM-dependent phosphorylation of ATF2 is required for the DNA damage response, Mol. Cell 18 (2005) 577–587.
[29] T. Akimoto, S.C. Pohnert, P. Li, M. Zhang, C. Gumbs, P.B. Rosenberg, R.S. Williams, Z. Yan, Exercise stimulates Pgc-1alpha transcription in skeletal muscle through activation of the p38 MAPK pathway, J. Biol. Chem. 280 (2005) 19587–19593.
[30] S.Y. Fuchs, I. Tappin, Z. Ronai, Stability of the ATF2 transcription factor is regulated by phosphorylation and dephosphorylation, J. Biol. Chem. 275 (2000) 12560–12564.
[31] R. Esterberg, T. Linbo, S.B. Pickett, P. Wu, H.C. Ou, E.W. Rubel, D.W. Raible, Mitochondrial calcium uptake underlies ROS generation during aminoglycoside-induced hair cell death, J. Clin. Investig. 126 (2016) 3556–3566.
[32] Y. Han, S. Ishibashi, J. Iglesias-Gonzalez, Y. Chen, N.R. Love, E. Amaya, Ca(2+)-Induced mitochondrial ROS regulate the early embryonic cell cycle, Cell Rep. 22 (2018) 218–231.
[33] Y.Q. Xiao, C.G. Freire-de-Lima, W.J. Janssen, K. Morimoto, D. Lyu, D.L. Bratton, P.M. Henson, Oxidants selectively reverse TGF-beta suppression of proinflammatory mediator production, J. Immunol. 176 (2006) 1209–1217.
[34] P.V. Usatyuk, S. Vepa, T. Watkins, D. He, N.L. Parinandi, V. Natarajan, Redox regulation of reactive oxygen species-induced p38 MAP kinase activation and barrier dysfunction in lung microvascular endothelial cells, Antioxidants Redox Signal. 5 (2003) 723–730.
[35] S. Murthy, J.L. Larson Casey, A.J. Ryan, C. He, L. Kobzik, A.B. Carter, Alternative activation of macrophages and pulmonary fibrosis are modulated by scavenger receptor, macrophage receptor with collagenous structure, FASEB J. 29 (2015) 3527–3536.
[36] S. Baldelli, K. Aquilano, M.R. Ciriolo, PGC-1alpha buffers ROS-mediated removal of mitochondria during myogenesis, Cell Death Dis. 5 (2014) e1515.
[37] J. St-Pierre, S. Drori, M. Uldry, J.M. Silvaggi, J. Rhee, S. Jager, C. Handschin,

K. Zheng, J. Lin, W. Yang, D.K. Simon, R. Bachoo, B.M. Spiegelman, Suppression of reactive oxygen species and neurodegeneration by the PGC-1 transcriptional coactivators, Cell 127 (2006) 397–408.
[38] R. Marcu, B.M. Wiczer, C.K. Neeley, B.J. Hawkins, Mitochondrial matrix Ca(2)(+) accumulation regulates cytosolic NAD(+)/NADH metabolism, protein acetylation, and sirtuin expression, Mol. Cell. Biol. 34 (2014) 2890–2902.
[39] S.C. Huang, B. Everts, Y. Ivanova, D. O'Sullivan, M. Nascimento, A.M. Smith, W. Beatty, L. Love-Gregory, W.Y. Lam, C.M. O'Neill, C. Yan, H. Du, N.A. Abumrad, J.F. Urban Jr., M.N. Artyomov, E.L. Pearce, E.J. Pearce, Cell-intrinsic lysosomal lipolysis is essential for alternative activation of macrophages, Nat. Immunol. 15 (2014) 846–855.
[40] J.C. Rodriguez-Prados, P.G. Traves, J. Cuenca, D. Rico, J. Aragones, P. Martin-Sanz, M. Cascante, L. Bosca, Substrate fate in activated macrophages: a comparison between innate, classic, and alternative activation, J. Immunol. 185 (2010) 605–614.
[41] G.J. van der Windt, B. Everts, C.H. Chang, J.D. Curtis, T.C. Freitas, E. Amiel, E.J. Pearce, E.L. Pearce, Mitochondrial respiratory capacity is a critical regulator of CD8+ T cell memory development, Immunity 36 (2012) 68–78.
[42] K. Lee, J. Kerner, C.L. Hoppel, Mitochondrial carnitine palmitoyltransferase 1a (CPT1a) is part of an outer membrane fatty acid transfer complex, J. Biol. Chem. 286 (2011) 25655–25662.
[43] L. Abu-Elheiga, W.R. Brinkley, L. Zhong, S.S. Chirala, G. Woldegiorgis, S.J. Wakil, The subcellular localization of acetyl-CoA carboxylase 2, Proc. Natl. Acad. Sci. U. S. A. 97 (2000) 1444–1449.
[44] K.L. Hoehn, N. Turner, M.M. Swarbrick, D. Wilks, E. Preston, Y. Phua, H. Joshi, S.M. Furler, M. Larance, B.D. Hegarty, S.J. Leslie, R. Pickford, A.J. Hoy, E.W. Kraegen, D.E. James, G.J. Cooney, Acute or chronic upregulation of mitochondrial fatty acid oxidation has no net effect on whole-body energy expenditure or adiposity, Cell Metabol. 11 (2010) 70–76.
[45] J.I. Odegaard, A. Chawla, Alternative macrophage activation and metabolism, Annu. Rev. Pathol. 6 (2011) 275–297.
[46] M.F. Allard, B.O. Schonekess, S.L. Henning, D.R. English, G.D. Lopaschuk, Contribution of oxidative metabolism and glycolysis to ATP production in hypertrophied hearts, Am. J. Physiol. 267 (1994) H742–H750.
[47] K.M. Havas, V. Milchevskaya, K. Radic, A. Alladin, E. Kafkia, M. Garcia, J. Stolte, B. Klaus, N. Rotmensz, T.J. Gibson, B. Burwinkel, A. Schneeweiss, G. Pruneri, K.R. Patil, R. Sotillo, M. Jechlinger, Metabolic shifts in residual breast cancer drive tumor recurrence, J. Clin. Investig. 127 (2017) 2091–2105.
[48] R.L. Wahl, K. Zasadny, M. Helvie, G.D. Hutchins, B. Weber, R. Cody, Metabolic monitoring of breast cancer chemohormonotherapy using positron emission tomography: initial evaluation, J. Clin. Oncol. 11 (1993) 2101–2111.
[49] J.H. Park, S. Vithayathil, S. Kumar, P.L. Sung, L.E. Dobrolecki, V. Putluri, V.B. Bhat, S.K. Bhowmik, V. Gupta, K. Arora, D. Wu, E. Tsouko, Y. Zhang, S. Maity, T.R. Donti, B.H. Graham, D.E. Frigo, C. Coarfa, P. Yotnda, N. Putluri, A. Sreekumar, M.T. Lewis, C.J. Creighton, L.C. Wong, B.A. Kaipparettu, Fatty acid oxidation-driven Src links mitochondrial energy reprogramming and oncogenic properties in triple-negative breast cancer, Cell Rep. 14 (2016) 2154–2165.
[50] R. Camarda, A.Y. Zhou, R.A. Kohnz, S. Balakrishnan, C. Mahieu, B. Anderton, H. Eyob, S. Kajimura, A. Tward, G. Krings, D.K. Nomura, A. Goga, Inhibition of fatty acid oxidation as a therapy for MYC-overexpressing triple-negative breast cancer, Nat. Med. 22 (2016) 427–432.
[51] K. Matsusue, M. Haluzik, G. Lambert, S.H. Yim, O. Gavrilova, J.M. Ward, B. Brewer Jr., M.L. Reitman, F.J. Gonzalez, Liver-specific disruption of PPARgamma in leptin-deficient mice improves fatty liver but aggravates diabetic phenotypes, J. Clin. Investig. 111 (2003) 737–747.
[52] T. Nakajima, Y. Kamijo, N. Tanaka, E. Sugiyama, E. Tanaka, K. Kiyosawa, Y. Fukushima, J.M. Peters, F.J. Gonzalez, T. Aoyama, Peroxisome proliferator-activated receptor alpha protects against alcohol-induced liver damage, Hepatology 40 (2004) 972–980.
[53] H.M. Kang, S.H. Ahn, P. Choi, Y.A. Ko, S.H. Han, F. Chinga, A.S. Park, J. Tao, K. Sharma, J. Pullman, E.P. Bottinger, I.J. Goldberg, K. Susztak, Defective fatty acid oxidation in renal tubular epithelial cells has a key role in kidney fibrosis development, Nat. Med. 21 (2015) 37–46.
[54] A.I. Tarasov, F. Semplici, M.A. Ravier, E.A. Bellomo, T.J. Pullen, P. Gilon, I. Sekler, R. Rizzuto, G.A. Rutter, The mitochondrial Ca2+ uniporter MCU is essential for glucose-induced ATP increases in pancreatic beta-cells, PLoS One 7 (2012) e39722.
[55] H. Lu, R.A. Forbes, A. Verma, Hypoxia-inducible factor 1 activation by aerobic glycolysis implicates the Warburg effect in carcinogenesis, J. Biol. Chem. 277 (2002) 23111–23115.
[56] H. Matsuoka, T. Arai, M. Mori, S. Goya, H. Kida, H. Morishita, H. Fujiwara, I. Tachibana, T. Osaki, S. Hayashi, A p38 MAPK inhibitor, FR-167653, ameliorates murine bleomycin-induced pulmonary fibrosis, Am. J. Physiol. Lung Cell Mol. Physiol. 283 (2002) L103–L112.
[57] P. Puigserver, J. Rhee, J. Lin, Z. Wu, J.C. Yoon, C.Y. Zhang, S. Krauss, V.K. Mootha, B.B. Lowell, B.M. Spiegelman, Cytokine stimulation of energy expenditure through p38 MAP kinase activation of PPARgamma coactivator-1, Mol. Cell 8 (2001) 971–982.
[58] I. Irrcher, V. Ljubicic, D.A. Hood, Interactions between ROS and AMP kinase activity in the regulation of PGC-1alpha transcription in skeletal muscle cells, Am. J. Physiol. Cell Physiol. 296 (2009) C116–C123.
[59] W. Assaily, D.A. Rubinger, K. Wheaton, Y. Lin, W. Ma, W. Xuan, L. Brown-Endres, K. Tsuchihara, T.W. Mak, S. Benchimol, ROS-mediated p53 induction of Lpin1 regulates fatty acid oxidation in response to nutritional stress, Mol. Cell 44 (2011) 491–501.
[60] D.N. Douglas, C.H. Pu, J.T. Lewis, R. Bhat, A. Anwar-Mohamed, M. Logan, G. Lund, W.R. Addison, R. Lehner, N.M. Kneteman, Oxidative stress attenuates lipid synthesis and increases mitochondrial fatty acid oxidation in hepatoma cells infected with hepatitis C virus, J. Biol. Chem. 291 (2016) 1974–1990.
[61] M.G. Rosca, E.J. Vazquez, Q. Chen, J. Kerner, T.S. Kern, C.L. Hoppel, Oxidation of fatty acids is the source of increased mitochondrial reactive oxygen species production in kidney cortical tubules in early diabetes, Diabetes 61 (2012) 2074–2083.
[62] C. He, A.J. Ryan, S. Murthy, A.B. Carter, Accelerated development of pulmonary fibrosis via Cu,Zn-superoxide dismutase-induced alternative activation of macrophages, J. Biol. Chem. 288 (2013) 20745–20757.
[63] H.L. Osborn-Heaford, A.J. Ryan, S. Murthy, A.M. Racila, C. He, J.C. Sieren, D.R. Spitz, A.B. Carter, Mitochondrial Rac1 GTPase import and electron transfer from cytochrome c are required for pulmonary fibrosis, J. Biol. Chem. 287 (2012) 3301–3312.
[64] N. Xie, H. Cui, J. Ge, S. Banerjee, S. Guo, S. Dubey, E. Abraham, R. Liu, G. Liu, Metabolic characterization and RNA profiling reveal glycolytic dependence of profibrotic phenotype of alveolar macrophages in lung fibrosis, Am. J. Physiol. Lung Cell Mol. Physiol. 313 (2017) L834–L844.